Manuscript submitted for publication in:

Spectrochimica Acta Part A: Molecular and Biomolecular Spectroscopy

Spectroscopic and theoretical studies of some 2-(methoxy)-2-[(4-substituted)-phenylsulfanyl]-(4'-substituted) acetophenones

Contents: 27 pages, 13 tables, 6 figures, 2 schemes, 2 supplementary tables, 9 supplementary figures and 1 supplementary scheme

***Corresponding author:**

Daniel N. S. Rodrigues

Conformational Analysis and Electronic Interactions Laboratory, Institute of Chemistry, University of São Paulo, P. O. Box 26077, 05513-970, São Paulo, SP, Brazil.

E-mail: dannoppper@gmail.com (D.N.S. Rodrigues)

Spectroscopic and theoretical studies of some 2-(methoxy)-2-[(4-substituted)-phenylsulfanyl]-(4'-substituted) acetophenones

Henrique J. Traesel,[a] Paulo R. Olivato,[a] Daniel N. S. Rodrigues,[a]* Jéssica Valença,[a] Alessandro Rodrigues,[b] JulioZukerman-Schpector,[c] Maurizio Dal Colle[d]

[a]*Conformational Analysis and Electronic Interactions Laboratory, Institute of Chemistry, University of São Paulo, CP 26077, 05513-970, São Paulo, SP, Brazil*

[b]*Department of Chemistry, Federal University of São Paulo, UNIFESP, 09972-270, Diadema, SP, Brazil,*

[c]*Department of Chemistry, Federal University of São Carlos, CP 676, 13565-905, São Carlos, SP, Brazil*

[d]*Dipartimento di Scienze Chimiche e Farmaceutiche, Università di Ferrara, 44121, Ferrara, Italy*

ABSTRACT:

The conformational analysis of some 2-(methoxy)-2-[(4-substituted)-phenylsulfanyl]-(4'-substituted) acetophenones was performed through infrared (IR) spectroscopic analysis of the carbonyl stretching band (ν_{CO}), supported by B3LYP/6-31+G(d,p) calculations and X-ray diffraction. Five (**1**-**5**) of the seven studied compounds (**1**-**7**) presented Fermi resonance (FR) on the ν_{CO} fundamental transition band. Deuteration of these compounds (**1a**-**5a**) precluded the occurrence of FR, revealing a ν_{CO} doubletfor all compounds in all solvents used. The computational results indicated the existence of three conformers (c_1, c_2 and c_3) for the whole series whose relative abundances varied with solvent permittivity. The higher ν_{CO} frequency c_1 conformer was assigned to the higher frequency component of the carbonyl doublet, while both c_2 and c_3 were assigned to the lower frequency one. Anharmonic vibrational frequencies and Potential Energy Distribution (PED) calculations of compound **3**

indicated that the combination band (cb) between the methyne δ_{CH} and one skeletal mode couples with the ν_{CO} mode giving rise to the FR on the c_2 conformer in vacuum and on the c_1 one in non-polar solvents. The experimental data indicated a progressive increase in c_1 conformer stability with the increase of the solvent dielectric constant, which is in good agreement with the polarizable continuum model (PCM) calculations. The higher ν_{CO} frequency and the stronger solvation of the c_1 conformer is a consequence of the repulsive field effect (RFE) originated by the alignment and closeness of the $C^{\delta+}=O^{\delta-}$ and $C^{\delta+}–O^{\delta-}$ dipoles. Finally, the balance between orbital and electrostatic interactions dictates the conformational preferences. X-ray single crystal analysis for compound **6** revealed the c_1 geometry in the solid state and its stabilization by C-H…O hydrogen bonds.

Keywords: Conformational analysis; infrared spectroscopy; Fermi resonance; theoretical calculations; solvent effect; X-ray diffraction; 2-(methoxy)-2-[(4-substituted)-phenylsulfanyl]-(4'-substituted) acetophenones.

1. INTRODUCTION

α-Thio-keto compounds constitute an important organic framework widely applied as intermediates in many synthetic transformations [1], and frequently used as building blocks in the synthesis of drugs and bioactive compounds [2]. In this context, α-keto thioacetals and their analogues are often used in various synthetic applications, such as in the preparation of complex intermediates [3] and bioactive natural products [4]. With the objective of exploring these themes we have been performing studies in searching for selective cyclooxygenase-2 (COX-2) enzyme inhibitors containing selenium-sulfur atoms [5–7], and in molecular docking studies [8] to understand the mechanism of its inhibition. The X-ray crystal and molecular structure of compound (**6**) was determined, described, and compared with those already published, such as 2-(4-chlorophenylsulfanyl)-2-methoxy-1-phenylethanone [9], 2-methoxy-2-(4-methylphenylsulfanyl)-1-phenylethanone [10], and 2-methoxy-2-(4-methoxyphenylsulfanyl)-1-phenylethanone [11].

In the last thirty years, the conformational analysis of several different carbonyl compounds performed by our research group, based on a number of spectroscopic (IR, UV, NMR, UPS and ETS) and X-ray studies supported by theoretical calculations, disclosed some relevant findings. The studies of some (α-alkylthio)- and (α-phenylthio)-acetones, acetophenones, *N,N*-diethylamides, esters, thioesters [12,13], *N*-methoxy-*N*-methyl amides [14], and *N*-methyl-δ-valerolactams [15], indicated that the simultaneous occurrence of the $n_S \rightarrow \pi^*_{CO}$, $\sigma_{C\text{-}S} \rightarrow \pi^*_{CO}$, and $\pi_{CO} \rightarrow \sigma^*_{C\text{-}S}$ orbital interactions is the main controlling factor that determines the preference of the *gauche* (*axial*) conformer(s) over the *cis* (*equatorial*) one(s).

The IR carbonyl stretching analysis of the α-(*p*-substituted-phenoxy)-*p*'-substituted acetophenones, X–C_6H_4–C(O)–CH_2–O–C_6H_4–Y (X and Y = NO_2, H, and OMe) [16], indicated the existence of *cis-gauche* rotational isomerism. The sum of the field (F), inductive (-Iσ), and mesomeric (M) effects in the *cis* rotamers of the derivatives with (X = H and OMe) for (Y = NO_2, H, and OMe) causes a similar carbonyl bond order, which accounts for the almost constant positive carbonyl frequency shifts observed. Additionally, for any Y substituent, the *gauche* conformers in the *p*-nitroacetophenones (X = NO_2) are more stable than the *cis* ones, while in the methoxyacetophenones (X = OMe) and acetophenones (X = H), the *cis* conformers are slightly more stable. This behavior was ascribed to the $\pi^*_{CO(LUMO)}/n_{O(OC6H4\text{-}Y)}$ orbital

interaction, which stabilizes the *gauche* conformers of the (X = NO_2) derivative to a larger extent than the (X = OMe and H) ones.

The experimental photoelectron spectra of the Me_2X (X = S and O) compounds indicated that both the n_S lone pair (8.71 eV) and the σ_{C-S} orbital (11.28 eV) [17] ionization energies are lower than those of the n_O lone pair (10.04 eV) and the σ_{C-O} orbital (11.91 eV) [17]. In addition, the σ^*_{C-S} (3.25 eV) [18] electron-affinity energy is higher than that of σ^*_{C-O} (6.0 eV [19] or 4.2 eV [20,21]). Therefore, as shown in our previous papers [12–16], then $_{X\rightarrow}\pi^*_{CO}$, $\sigma_{C-X\rightarrow}\pi^*_{CO}$, $\pi_{CO\rightarrow}\sigma^*_{C-X}$ interactions are stronger in the *gauche* (*axial*) conformer(s) of the α-thio-carbonyl compounds (X = S) than for the analogous conformer in the α-oxa-acetophenones (X = O).

Stimulated by the above discussion, this study reports the conformational analysis and the electronic interactions of some mixed acetophenones bearing both the phenylthio- and the methoxy- substituents in the α position. This study analyses the 2-(methoxy)-[(4-substituted)-phenylsulfanyl]-(4'-substituted)acetophenones **1-7** (Scheme 1). The occurrence of conformational isomerism is investigated through the ν_{CO} infrared band decomposition method in solvents of increasing dielectric constant. The obtained spectroscopic results are supported by theoretical calculations and X-ray diffraction data. The occurrence of unexpected Fermi resonance is fully experimentally resolved and also discussed in terms of the normal coordinate analysis.

In particular, these compounds became spectroscopically interesting as the α substituents are expected to compete for the *syn-clinal* or *anti-clinal* (*gauche*) and *syn-periplanar* (*cis*) geometries with respect to the carbonyl group, due to differences in the orbital and electrostatic interactions that stabilizes the conformers. Finally, this work is an extension of recent conformational studies on the 2-(phenylselanyl)-2-(methoxy)-acetophenones, 2-(phenylseleno)-2-(ethylsulfanyl)-acetophenones and their mono- and di-oxygenated derivatives [5–7,22].

2. EXPERIMENTAL SECTION

2.1 Materials

All solvents for IR measurements were spectrograde and were used without further purification. The 2-(methoxy)-[(4-substituted)-phenylsulfanyl]-(4'-substituted) acetophenones **1–7** are new compounds and were prepared according to the literature [23] as follows: a THF solution of 2-(methoxy)-4'-substituted-acetophenone was slowly added to a stirred solution of LDA in THF at 195 K. After 30 minutes, a solution of 1,2-

bis(4-substituted-phenyl)-disulfide with HMPA [24,25] in THF was added dropwise, with immediate discoloration of the reactant. Water was added, and crude product extracted with ethyl ether or dichloromethane after the reaction mixture reached room temperature (*ca.* 3 h). The organic layer was washed with a saturated NH_4Cl solution till neutral pH and dried over anhydrous magnesium sulphate. The obtained crude product was purified by flash chromatography on silica gel, and after solvent evaporation a solid was obtained.

The corresponding α-methyne deuterated compounds **1a**–**5a** were obtained from an adaptation of the literature procedure [26] as follows: 5 mg of anhydrous K_2CO_3 was added to a stirring solution of 2-(methoxy)-2-(4-substituted-phenylsulfanyl) acetophenone in a 50% methanol-d_4 (CD_3OD) and $CDCl_3$ solution at room temperature. The progress of the isotopic substitution was followed through ^1H NMR. When the progress of hydrogen/deuterium exchange reached an equilibrium of *ca*. 95% (*ca*. 30 minutes) the mixture was centrifuged. The organic layer was then carefully collected and filtered through a thin pad of Celite® 545 (SiO_2), giving the 2-deutero-2-(methoxy)-2-(4-substituted-phenylsulfanyl) acetophenones **1a**–**5a**. The reagents 2-methoxy-acetophenone (Sigma-Aldrich), 2-methoxy-(4'-methoxy)-, and 2-methoxy-(4'-chloro)-acetophenones (Novel Chemical Solutions) were commercially available. Suitable crystals of **6** for X-ray analysis were obtained by vapor diffusion from chloroform/*n*-hexane at 283 K. The ^1H and ^{13}C NMR data and elemental analysis for compounds **1**–**7** are presented in Table 1.

2.2 IR Spectroscopy

The IR spectra for the fundamental carbonyl region (1800-1600 cm^{-1}) were recorded with a FTIR Michelson Bomem MB100 spectrometer with 1.0 cm^{-1} resolution at a concentration of 1.0 x 10^{-2} mol dm^{-3} in *n*-hexane, carbon tetrachloride, chloroform, dichloromethane, and acetonitrile solutions using a 0.519 mm sodium chloride cell. The spectra for the carbonyl first overtone region (3600-3100 cm^{-1}) were recorded in a carbon tetrachloride solution (1.0 x 10^{-2} mol dm^{-3}) using a 1.00 cm quartz cell. The overlapping carbonyl bands (fundamental and first overtone) were deconvoluted using the Grams/32 curve fitting program version 4.04 [27]. The relative intensities and the conformer populations for the title compounds **1-7** and **1a-5a** in the referred solvents were estimated from the percentage of the integrated absorbance $B = \int_{\text{band}} \ln(I_0/I)_\nu d\nu$

(in cm^{-1}) for each resolved carbonyl multiplet (doublet or triplet) component assuming equal integrated molar absorption coefficient $\overline{A} = \frac{1}{cl}\int_{band} \ln(I_0/I)_\nu d\nu$ (km mol^{-1}) for all the conformers [28].

2.3 NMR Spectroscopy

^1H NMR and ^{13}C NMR spectra were recorded on a Bruker DRX 500 spectrometer operating at 500.130 and 125.758 MHz, respectively, for 0.1 mol dm^{-3} solutions in $CDCl_3$. ^1H and ^{13}C chemical shifts are reported in ppm relative to the internal standard TMS.

2.4 X-ray Measurements

The X-ray diffraction measurements for the colorless crystal of **6** were performed at 293 K on a Bruker SMART APEX II CCD diffractometer fitted with MoKα radiation. The data set was corrected for absorption based on multiple scans [29] and reduced using standard methods [30]. The structure was solved by direct methods [31] and refined on F^2 (anisotropic displacement parameters, C-bound H atoms in the riding model approximation) using the SHELXL2014/6 program [32] through the WinGX Interface [33]. Crystal data and refinement details are collated in Table 2. The molecular structure diagram was drawn with ORTEP-3 for Windows [33]. Crystallographic data for the structural analysis have been deposited with the Cambridge Crystallographic Data Centre as CCDC 1859035. Copies of this information may be obtained free of charge on application to CCDC, 12 Union Road, Cambridge CB2 1EZ, UK (fax: 44 1223 336 033; e-mail: deposit@ccdc.cam.ac.uk or www: http://www.ccdc.cam.ac.uk).

2.5 Theoretical Calculations

The conformational search was performed using Monte Carlo's method in HF/STO-3G theory level with Spartan '06 software [34]. The obtained conformer geometries were used as initial inputs in all calculations carried out at 298 K using the methods and basis sets implemented in the Gaussian package of programs (G09-D01) [35] with a hybrid Hartree-Fock density functional B3LYP method [36–38] and the 6-31+G(d,p) basis set. Full geometrical optimizations and analytical harmonic vibrational frequency calculations were performed on the most stable conformers. Frequency analysis was carried out to verify the nature of the minimum state of the stationary

points and to calculate the zero-point vibrational energy (ZPVE) corrections. To estimate the solvation effects on the relative stability of the most relevant conformers, calculations were conducted on the optimized structures using the polarizable continuum model (PCM) [39,40]. Due to the lack of symmetry of the three conformers found (C_1 point group), the thermodynamic probability factor was the same ($\omega = 2$) for all of them. The NBO 6.0 program [41] was used as implemented in the Gaussian 09 package, and the reported NBO delocalization energies (E2) were those given by second-order perturbation theory. The partial atomic charges were calculated using the charges from electrostatic potentials using a grid-based method (ChELPG) [42]. In order to compare the performance of B3LYP functional with others that include dispersion energy corrections, M06-2X [43] and B3LYP-D3 [44] calculations along with the 6-31+G(d,p) basis set were performed for compound **3**, both in gas and in condensed phase (PCM) (Tables S1 and S2).

The anharmonic vibrational frequency calculations were obtained with the inclusion of the anharmonic potential as denotedin the Gaussian 09 revision A02 [45] program. The analysis of anharmonic frequencies along with a search for coupling vibrational modes calculations were performed for compound (**3**), representative for the series, in order to check if Fermi resonance operates in the system. The obtained fundamental modes of vibrations were analyzed in the potential energy distribution (PED) terms using theVEDA [46] program.

3. RESULTS AND DISCUSSION

3.1 Infrared Analysis

Table 3 lists the stretching frequencies and the integrated absorbance percentages of the analytically resolved components of the carbonyl band for the 2-(methoxy)-[(4-substituted)-phenylsulfanyl]-(4'-substituted) acetophenones **1**-**7** in solvents of increasing relative permittivity [47], from *n*-hexane ($\varepsilon = 1.9$) to acetonitrile ($\varepsilon = 38$), except for compounds **1**, **4**, and **5**, which are insoluble in *n*-hexane. It should be pointed out that a ν_{CO} triplet was found in solvents of low polarity for compounds **2** and **3** (in *n*-hexane) and **1**-**5** (in carbon tetrachloride) in the fundamental region, but not in the first overtone region, for which only a doublet is present. Moreover, for **1**-**3** as the solvent polarity increases, from $CHCl_3$ to CH_3CN, only a doublet is detected unless for **1** in CH_2Cl_2 where a triplet occurs. As for **4** and **5**, a triplet is present in the polar solvents $CHCl_3$, CH_2Cl_2 and CH_3CN. For compounds **6** and **7** bearing 4'-substituents in

the acetophenone moiety, only doublets are observed in all solvents, in the fundamental region, as well as in the first overtone, in CCl_4. The solvent effect on the carbonyl band components for compounds **1**-**7** is illustrated in Figures 1 and S1-S4.

The occurrence of three carbonyl band components in the fundamental region (carbon tetrachloride) and only a doublet in the first overtone region for **1**-**5** is indicative of the occurrence of the Fermi resonance in the fundamental transitions [48,49] (see below). On the other hand, the doublet found in all solvents in the fundamental region for **6** and **7** was reproduced in the first overtone region (in carbon tetrachloride). Moreover, the occurrence of two carbonyl band components in the first overtone at frequencies twice those of fundamental transition, minus *ca.* 18 cm^{-1} (twice the mechanical anharmonicity $\omega_e\chi_e$) [28,48], and intensity ratios comparable to those of the fundamentals is indicative of the presence of at least two conformers. This behavior rules out the existence of the FR in the fundamental transition of the ν_{CO} mode [48,49].

It is well known that the isotopic substitution of one or more atoms in a molecule can significantly change the vibrational levels, breaking the accidental degeneracy and destroying the FR phenomena [26,50,51]. In fact, the classical example of the FR is the carbonyl stretching regionin the IR spectra of the cyclopentanone, which shows a doublet in solution, but α, α, α', α'- cyclopentanone-d_4 destroys the FR, displaying only a single carbonyl stretching band.

Therefore, in this work we undertook the deuteration of the α methyne hydrogen atom of compounds **1**-**5** obtaining the 2-(deutero)-2-(methoxy)-2-(4-substituted-phenylsulfanyl) acetophenones, whose carbonyl region is presented in Table 4. This table shows the presence of only carbonyl doublets in the fundamental region for **1a**-**5a** in all solvents, and the occurrence of a doublet in the first overtone region in CCl_4, with each component frequency twice that of fundamental transition minus *ca.* 17 cm^{-1} (twice the mechanical anharmonicity $\omega_e\chi_e$) and intensity ratios close to those of the fundamentals. This behavior is similar to that of compounds **6** and **7**, being indicative of the presence of at least two conformers in solution. In addition, the intensity of the higher frequency component for **1a**-**5a** increases with respect to the lower frequency as the solvent polarity increases, as shown in Figures 2 and S5-S8. Likewise, the analogous solvent effect is observed for derivatives **6** and **7** (Figure 3).

The comparison between carbonyl stretching IR bands of compounds (**1**-**5**) (Table 3) with the corresponding deuterated derivatives (**1a**-**5a**) (Table 4) indicates the

absence of the highest triplet frequency component for compounds **2**, **3** in *n*-C_6H_{14}, **1**-**5** in CCl_4, **1** in CH_2Cl_2, and **4** and **5** in $CHCl_3$, CH_2Cl_2 and CH_3CN.

The disappearance of this component in the deuterated derivatives suggests the occurrence in compounds **1**-**5** of the anharmonic Fermi resonance between the carbonyl stretching fundamental of one conformer (the intense middle frequency triplet component) and a combination band involving the C–H deformation and skeletal modes (the less intense highest frequency component) (see Section 3.3). The frequencies of the unperturbed transitions can be estimated from the experimental shifted values through the following Equation (I) [28,52]:

$$\nu^0_{n,m} = \frac{\nu_n+\nu_m}{2} \pm \frac{\nu_n-\nu_m}{2}\left(\frac{\rho-1}{\rho+1}\right) \quad \text{(I)}$$

where ν°_n and ν°_m are the unperturbed corrected frequencies, ν_n and ν_m are the observed frequencies, and ρis the intensity ratio A_n/A_m expressed in absorbance at the referred band maxima. All of the relevant data is collected in Table 5 for **1**-**5**, along with the higher doublet frequency component of the deuterated derivatives (**1a**-**5a**) in solution.

The large frequency shift ($\Delta\nu_{m,n}=\nu_m-\nu_n$, *ca.*10 cm^{-1}) observed in non-polar solvents is a consequence of the closeness of the unperturbed transitions ($\Delta\nu^\circ_{m,n}$ *ca.* 3.5 cm^{-1}). On the contrary, in polar solvents the Fermi resonance slightly affects the excited states, thus leading to a negligible splitting, that is $\Delta\nu_{m,n}$ of *ca.* 12 cm^{-1} in comparison with the unperturbed one $\Delta\nu^\circ_{m,n}$ *ca.* 11 cm^{-1}. As expected, the Fermi coupling coefficient W for compound **4**, obtained with Equation (II) [50], is larger in the non-polar solvent CCl_4 (W = 4.8 cm^{-1}) and smaller in the polar solvent CH_3CN (W = 3.8 cm^{-1}).

$$\Delta^2_{(n,m)} = \Delta^2_{0(n,m)} + 4W^2 \quad \text{(II)}$$

These behaviors are clearly summarized in the bar diagrams in Schemes 2 and S1. Additionally, both Table 5 and Scheme 2 show that the higher doublet frequency component of the deuterated compounds displays ν_{CO} frequency close or slightly lower (due to some mass effect) to that of the lower computed unperturbed ν°_m frequency. This proximity is further evidence that the lowest doublet frequency corresponds to the fundamental $\nu^\circ_{m(CO)}$ transition and the higher one (ν°_n) is due to the unperturbed combination band.

3.2 Geometries and Properties

The relevant DFT data, calculated at the B3LYP/6-31+G(d,p) level, of the optimized geometries for compounds **1**-**7** are reported in Table 6, along with the vibrational frequencies of the minimum energy conformations and the X-ray dihedral angles for **6**.

The calculations indicate the existence of three distinct conformers, which assume a *synperiplanar* (c_1, $\alpha \approx 25°$) and *anti-clinal* ($c_2 \approx c_3$, $\alpha \approx 130°$) geometry between the C─O and C=O groups, and an*anti-clinal* orientation between the C─S and C=O groups, with $\alpha' \approx 101°$ for c_1 and c_2 and $\alpha' \approx 111°$ for c_3, for the whole series. The computed structures of the c_1, c_2, and c_3 conformers of **3**, taken as representative of the series **1**-**7**, are reported in Figure 4.

The c_2 conformers are the most stables in the series (**1**-**7**), and their relative abundances increase from compound **1** (74.8%) to compound **7** (86.7%) (Table 6). On the contrary, the relative population of the second stable c_3 conformer and the less stable c_1 one decreases on going from compound **1** (c_3 20.7%, c_1 4.5%) to **7** (c_3 11.1%, c_1 2.1%). Moreover, the c_1 conformers have the highest carbonyl frequency in the series, while the c_2 and c_3 ones have similar low values. Therefore, the less intense carbonyl doublet component at high frequency in the IR spectra for **6** and **7** (Table 3), as well as for **1a**-**5a** (Table 4) in the non-polar solvents *n*-C_6H_{14} and CCl_4, could be reasonably ascribed to the c_1 conformer. Consequently, the intense component at low frequency corresponds to both the c_2 and c_3 conformers. These assignments are fully supported by the PCM calculations (Table 7), which indicate an increase in the c_1 conformer relative abundance and the concomitant decrease in the c_2 and c_3 relative abundances, as the solvent polarity increases, which is in agreement with the experimental behavior in solution.

This experimental and theoretical trend can be rationalized taking into account the suitable geometry of the c_1 conformer which favor, in solvent of increasing polarity, a local stabilizing solvation of the *quasi* parallel $C^{\delta+}=O^{\delta-}$ and $C^{\delta+}–O^{\delta-}$ dipoles.

Calculations at the same level have been performed for the α-methyne deuterated analogue **3a**, representative of the **1a**-**5a** series. As expected, the c_1, c_2, and c_3 conformers of **3a** exhibit the same geometries and dipole moments of the corresponding non-deuterated compound **3**, with negligible difference in the relative energies. Furthermore, their $\nu_{CO(D)}$ frequencies (Table 6) were lowered by *ca*. 2 cm^{-1}

with respect to the corresponding frequencies in compound **3** due to small mass effects of the substituted deuterium atom.

In order to check if the inclusion of dispersion energy corrections would significantly change the properties of the conformers, B3LYP-D3 and M06-2X calculations along with the 6-31+G(d,p) basis set were performed for **3**, taken as representative for the whole series, both in gas and in condensed phase (PCM). The molecular geometries, carbonyl frequencies and relative energy trends in the gas phase, presented in Table S1, are quite similar to those obtained at B3LYP/6-31+G(d,p) level (Table 6). Furthermore, computations in condensed phase (PCM), carried out at the above mentioned levels of theory (Table S2), lead to the same trend found at B3LYP/6-31+G(d,p) level (Table 7) which closely reproduces the experimental data (Table 4) conducting to the same general conclusions.

3.3 Anharmonic Frequencies and Potential Energy Distribution Analyses

Detailed anharmonic frequencies studies were carried out at the B3LYP/6-31+G(d,p) level for the representative compound **3** in order to identify the vibrational modes that give rise to the combination band, which interacts with the ν_{CO} mode causing the Fermi resonance. The results indicate that in the c_2 conformer the carbonyl symmetric stretching excited level can be mixed with the excited vibrational state of a combination band involving the α hydrogen bending ($\delta_{C3\text{-}H4}$) and a skeletal mode and that this interaction is responsible for the calculated FR frequency splitting at 1709.0 cm^{-1} and 1696.1 cm^{-1}, respectively (Table 8). It is noteworthy that twice the mechanical anharmonicity ($2\omega_e\chi_e$) calculated (*ca.* 19.6 cm^{-1}) is in line with the experimental findings (*ca.* 18 cm^{-1}).

The computational results indicate that the FR occurs on the c_2 conformer, which is in disagreement with the experimental data that points to the higher frequency c_1 one. This discrepancy could be related to a solvent effect (see below).

To better understand the nature of the vibrational modes responsible for the interaction and how they couple each other, PED analysis was performed [46] for all conformers of compound **3** (Table 9).

For the three conformers, the vibrational mode 15 assigned as ν_{CO} (Tables 8 and 9) is mainly composed by the $\nu_{C1=O2}$ coordinate (≈ 88%) in the range of 1761-1736 cm^{-1}.

For the c_1 conformer, the mode 32 at ν = 1273.1 cm^{-1} is largely characterized by a torsion involving the H4–C3–O5–C6 group (25%) and a stretching of the C2–C22

bond (18%). On the contrary, the skeletal mode 72 at ν = 430.3 cm^{-1} consists of the mixing of four relevant coordinates, which is an out of plane phenacyl ring vibration (17%), several complex bending movements that include the methoxy carbon atom, the carbonyl and the phenacyl ring groups (13%), and finally two displacements involving the S-phenyl ring (11% for each mode). The characteristic coordinates suggest that the $\delta_{C3\text{-}H4}$ mode and the skeletal mode could be mechanically coupled along the C6–O5–C3(H4)–C2–C22 moiety.

It should be noted that thesignificant contribution of the H4 hydrogen atom to the $\delta_{C3–H4}$ mode implies that its frequency should be lowered with deuterium substitution, thus inhibiting the Fermi resonance, as verified for compounds **1a**-**5a**. Moreover, the phenacyl ring contribution to the skeletal mode suggests that the corresponding frequency can differ in the *mono*- or in the *para*-substituted derivatives and, consequently, the combination band frequency could be unsuitable for the occurrence of the Fermi resonance. That is the case for the *para*-substituted compounds **6** and **7**, for which the FR was not detected.

Table 9 indicates that the $\delta_{C–H}$ bending does not contribute to the 32 mode for the c_2 conformer. Nonetheless, this mode mainly involves the asymmetrical stretching $\nu_{C2–C22}$-$\nu_{C2–C3}$, which may couple mechanically with the $\nu_{C2–C22}$ coordinate of the skeletal mode. On the contrary, the $\delta_{C–H}$ and the skeletal modes in the c_3 conformer are composed of coordinates that preclude any mechanical coupling.

It is well known that an increase in the dielectric constant of the media lowers the ν_{CO} frequency [49,53] and increases the combination band frequency [53,54], mostly due to the δ_{CH} mode [26]. Table 10 reports the anharmonic unperturbed frequencies, calculated in vacuum and in two solvents of distinct polarities, of the three modes responsible for the FR, together with the frequency difference (Δν) between the combination band (32+72) and the ν_{CO} one. The large Δν for the c_1 conformer in vacuum and in the polar solvent CH_3CN (69.5 and -33.7 cm^{-1}, respectively), as well as for c_2 in CH_3CN (-53.4 cm^{-1}), accounts for the experimental absence of FR. On the contrary, the small Δν values for c_1 in the non-polar solvent CCl_4 (-5.8 cm^{-1}) and for c_2 (6.3 cm^{-1} in vacuum) allow its occurrence. These conclusions are in line with the experimental findings for the c_1 conformerin CCl_4 ($\Delta\nu° = -3.1$ cm^{-1}, Table 5) and with the calculations in vacuum for the c_2 one. Nevertheless, the Δν value of -11.5 cm^{-1} for the c_2 conformer in CCl_4, which is almost twice than that for the c_1 one, suggests that a weaker FR should be expected, although not detected experimentally.

As for the *c3* conformer, although there is a small Δν value in CH_3CN (-5.1 cm^{-1}), the FR is precluded in any solvent as a consequence of the lack of mechanical coupling between the δ_{C-H} and the skeletal modes, as evidenced by the PED analysis.

3.4 Short Contacts and Natural Orbital Analyses

Tables 11, 12, and 13 report the ChELPG charges, the interatomic distances of selected atoms, and NBO energies of selected orbital interactions, respectively, for the three conformers of compounds **1**-**7** calculated at the B3LYP/6-31+G(d,p) level.

The strongest orbital interactions for the three conformers arethe following: a) the conjugative $\pi_{C22=C31} \rightarrow \pi^*_{C2=O1}$ at mean energy values for all the conformers of *ca.* 22.2 kcal mol^{-1} for **1**-**5** and **7** and *ca.* 2 kcal mol^{-1} more for **6** due to the mesomeric effect of the 4'-substituent (Y = OMe); b) the $Lp_{O1} \rightarrow \sigma^*_{C2-C3}$ and $Lp_{O1} \rightarrow \sigma^*_{C2-C22}$ through bond coupling interactions [55], almost constant for each conformer in the series **1**-**7**, at mean energy values of *ca*. 22.1 kcal mol^{-1} and 19.4 kcal mol^{-1}, respectively. The *c1* and *c2* conformers are largely stabilized by the $Lp_{O5} \rightarrow \sigma^*_{C3-S10}$ interaction, which occurs for the suitable β dihedral angle (*ca*. 163°), which allows the $O_{(5)}$ lone pair to lie almost parallel to the antibonding σ^*_{C3-S10} orbital. This interaction is replaced in the *c3* conformers by the equivalent $Lp_{O5} \rightarrow \sigma^*_{C2-C3}$ one, which has a negligible effect on the *c1* and *c2* conformers. The sum of the two interactions stabilizes the *c1* and *c2* conformers (*ca*. 17.2 kcal mol^{-1}) more than the *c3* ones (*ca*. 10.6 kcal mol^{-1}). The analogous $Lp_{S10} \rightarrow \sigma^*_{C3-O5}$ and the weak $Lp_{S10} \rightarrow \sigma^*_{C2-C3}$ interactions, which occur when the β' dihedral angles have the proper values to force the S(10) lone pair to be parallel to the σ^*_{C3-O5} orbital, stabilize the three conformers to the same extent (8.5 kcal mol^{-1}). An effect of the unsuitable β and β' angles is the weakening of the $LP_{S10} \rightarrow \pi^*_{O1=C2}$ and $LP_{O5} \rightarrow \pi^*_{O1=C2}$ superjacent orbital interactions [56], whose sum contributes to the conformers stabilization byonly *ca*. 2.3 kcal mol^{-1} for *c2* and *ca*. 1.6 kcal mol^{-1} for *c1* and *c3*.

Additionally, the *quasi-antiperiplanar* geometry of the $C_{(3)}$–$S_{(10)}$ and $O_{(5)}$–$C_{(6)}$ bonds in the *c3* conformers allows the simultaneous weak interactions $\sigma_{C3-S10} \rightarrow \sigma^*_{O5-C6}$ and $\sigma_{O5-C6} \rightarrow \sigma^*_{C3-S10}$ for a total energy of *ca*. 4.7 kcal mol^{-1}.

The $Lp_{S10} \rightarrow \pi^*_{C11=C12}$ conjugation, whose energy is modulated by the γ' dihedral angle values, mainly stabilizes the *c1* and *c2* conformers (γ' *ca*. 60°) by a mean value of *ca*. 6.8 kcal mol^{-1} for compounds **3**-**7** and *ca*. 3.3 kcal mol^{-1} for derivatives **1** and **2**,

which have an electron-donor substituent at the *para* position of the phenylthio ring. The unsuitable γ' dihedral angle of *ca.* 110° for the c_3 conformers in the whole series reduces this interaction to just *ca.* 1.8 kcal mol^{-1} in **3**-**7** and 1.4 kcal mol^{-1} in **1**-**2**.

The orbital interactions $\pi_{C2=O1} \rightarrow \sigma^*_{C-Y}$ and $\sigma_{C-Y} \rightarrow \pi^*_{O1=C2}$ (Y = O or S), which are stronger for (Y = S) for the favorable overlap of the involved orbitals, are maximized as the α or α' torsional angles approach 90°. The energies of the $\sigma_{C3-S10} \rightarrow \pi^*_{O1=C2}$ and the $\pi_{C2=O1} \rightarrow \sigma^*_{C3-S10}$ orbital interactions decrease smoothly from the c_1 conformer (*ca.* 5.7 and 2.4 kcal mol^{-1}, respectively) to the c_3 one (*ca.* 4.3 and 1.8 kcal mol^{-1}, respectively), in line with the increase inthe α' dihedral angle from *ca.* 100° to 110°. The corresponding $\sigma_{C3-O5} \rightarrow \pi^*_{O1=C2}$ and $\pi_{C2=O1} \rightarrow \sigma^*_{C3-O5}$ interactions involving the oxygen atom show the opposite trend, *i.e.* an energy increase on going from the c_1 conformers to the c_3 ones. The former has a minor effect for all conformers (≤ 1.0 kcal mol^{-1}) as their α dihedral angles diverge from the optimal value of 90°, while the energy of the latter decreases from *ca.* 2.3 kcal mol^{-1} for c_3 to 1.9 kcal mol^{-1} for c_2 and to 0 kcal mol^{-1} for c_1.

The anomeric effect $LP_{O5} \rightarrow \sigma^*_{C3-H4}$ stabilizes the three conformers by *ca.* 3.4 kcal mol^{-1} for the whole series. The $O^{\delta-}{}_5 \cdots H^{\delta+}{}_{32}$ and $S^{\delta-}{}_{10} \cdots H^{\delta\delta+}{}_7$ hydrogen bonds were assessed (Table 12) by the $LP_{O5} \rightarrow \sigma^*_{C31-H32}$ and $LP_{S10} \rightarrow \sigma^*_{C6-H7}$ interactions, at a mean stabilization energy of *ca.* 0.8 kcal mol^{-1} for c_2 and c_3 and 0.7 kcal mol^{-1} for c_1 and c_2, respectively. The c_2 and c_3 conformers are electrostatically stabilized by the contact $O^{\delta-}{}_1 \cdots H^{\delta+}{}_4$, *ca.* -0.30 Å shorter than the sum of the van der Waals radii (ΣvdWr), while the c_3 one is weakly stabilized through the contact $S^{\delta-}{}_{10} \cdots H^{\delta+}{}_{32}$, *ca.* -0.05 Å shorter than the ΣvdWr.

The sum of the NBO orbital interactions (ΣE) for compounds **3**-**7** shows that the c_1 and c_2 conformers are stabilized almost to the same extent (*ca.* 112.1 kcal mol^{-1}), while the c_3 conformer is less stabilized by *ca.* 6.8 kcal mol^{-1}. At first sight, this difference could be ascribed to the $LP_{O5} \rightarrow \sigma^*_{C3-S10}$ and $LP_{O5} \rightarrow \sigma^*_{C2-C3}$ orbital interactions, which favour the c_1 and c_2 conformers over the c_3 one by just *ca.* 6.6 kcal mol^{-1}. Nevertheless, the average ΣE for the c_1 and c_2 conformers in the derivatives **1** and **2** is higher by only *ca.* 3.7 kcal mol^{-1} than the ΣE for the c_3 ones. This minor stabilization is partially related to the decrease from *ca.* 6.8 kcal mol^{-1} (compounds **3**-**7**) to *ca.* 3.3 kcal mol^{-1} (**1** and **2**) of the $LP_{S10} \rightarrow \pi^*_{C11=C12}$ conjugation energy for c_1 and c_2, caused by the electron–donor substituent at the *para* position of the phenylthio ring. Analogously, this

conjugation energy decreases from 1.8 kcal mol^{-1} to 1.4 kcal mol^{-1} for the c_3 conformers.

The short contact $O^{\delta-}(1)_{CO}\cdots O^{\delta-}(5)_{OMe}$, which uniquely occurs in the c_1 conformer (Table 12), gives rise to a strong repulsive destabilizing field effect (RFE) [49] between the $C^{\delta+}=O^{\delta-}$ and $C^{\delta+}\text{-}O^{\delta-}$ dipoles that induces a decrease in the carbonyl oxygen charge (Table 11). The concomitant increase in the $LP_{O1}\rightarrow\sigma^*_{C2-C3}$ delocalization energy by *ca*. 2.3 kcal mol^{-1} and the decrease in the $\pi_{C22=C31}\rightarrow\pi^*_{C2=O1}$ conjugative one by about the same amount (2.5 kcal mol^{-1}) for the c_1 conformers with respect to the c_2 and c_3 ones, lead to an increase in the carbonyl bond order and thus to higher ν_{CO} frequency.

As discussed, the strong repulsive effect between the $C^{\delta+}=O^{\delta-}$ and $C^{\delta+}\text{-}O^{\delta-}$ dipoles significantly destabilizes the c_1 conformer. Therefore, the high stability of the c_2 conformer compared to the c_1 and c_3 ones in the gas phase (Table 6) is likely related to a balance between the simultaneous occurrence of orbital delocalization energies and coulombic repulsive interactions.

3.5 X-Ray Diffraction

Relevant crystallographic information and final refinement parameters for **6** are given in Table 2. The ORTEP view of the asymmetric unit of **6** is shown in Figure 5 with atom labelling.

Table 4 shows that the geometry of compound **6** in the solid phase is quite equivalent to those previously studied for compounds **1** [7], **2** [6] and **3** [5]. In fact, to obtain the largest energy gain due to dipole moment coupling in the crystal, the molecules assume the least stable conformation (c_1) in the gas phase, as evidenced by the almost coincident values of the torsional α-ϕ' angles, whose $C^{\delta+}=O^{\delta-}$ and$C^{\delta+}\text{–}O^{\delta-}$ dipoles are *quasi*-parallel. It should be pointed out that the intramolecular contact $S_{10}\cdots H_7$ (hydrogen bond), shorter than the ΣvdWr (Δl = -0.13 Å) as in the gas phase, also contributes to stabilization of the (c_1) conformer in the solid phase of **6** (Table 12).

Figure 6 shows that compound **6** is stabilized in the crystal through the following two C–H…O interactions: C6–H7…O1^{i} (H…O = 2.60 Å, C–H…O = 123^{o}) and C33–H34…O5^{ii} (H…O = 2.56 Å, C–H…O = 129^{o}). Symmetry operations: i = x, 1+y, z and ii = x, 1.5-y, 0.5+z.

4.CONCLUSIONS

The conformational preferences of the 2-(methoxy)-2-[(4-substituted)-phenylsulfanyl]-(4'-substituted) acetophenones [Y-C_6H_4-C(O)-CH(O-CH_3)-S-C_6H_4-X] have been determined by ν_{CO} IR analysis and theoretical calculations at the B3LYP/6-31+G(d,p) level for compounds **1**-**7**. The ν_{CO} fundamental transition region of the spectra for compounds **1**-**5** (Y = H) suggests the occurrence of the Fermi resonance, confirmed by the lack of correspondence between the fundamental and first overtone bands profiles in non-polar solvents. The deuteration of the methyne hydrogen (**1a**-**5a**) inhibits the FR and indicated that the resonance takes place between the middle frequency ν_{CO} component of one conformer and the highest frequency one assigned to a combination band. The IR spectra of compounds **1a**-**5a**, **6**, and **7** revealed a ν_{CO} doublet, whose higher frequency component intensifies as the dielectric constant of the media increases. The theoretical data indicated the presence of three stable conformers (c_1, c_2 and c_3), which is in good agreement with the experimental spectra. PCM calculations showed that the higher ν_{CO} frequency c_1 conformer is stabilized as the solvent dielectric constant increases, while the relative populations of both the most stable c_2 and the c_3 one decreases. Since the c_2 and c_3 conformers ν_{CO} frequencies are almost coincident, they are both ascribed to the lower frequency component of the experimental IR ν_{CO} band.

Anharmonic and PED calculations for compound **3** indicate that the FR should occur on the c_2 conformer in vacuum and on the c_1 one in non-polar solvents, and that the resonance couples the ν_{CO} mode with a combination band involving the δ_{C3-H4} methyne hydrogen bending (mode 32) and a skeletal vibration which includes the phenacyl ring (mode 72). These results are in line with the experimental data, as the deuteration of the methyne hydrogen (**1a**-**5a**) or the substitution at 4' position of the phenacyl ring (**6** and **7**) precludes the FR.

The three conformers assume an *anti-clinal* geometry between the C─S and C=O groups and a *synperiplanar* (c_1) and *anti-clinal* (c_2 and c_3) orientation of the C─O and C=O groups, for the whole series.

The sum of the delocalization energies (NBO) of theselected orbitals stabilizes the c_1 and c_2 conformers almost to the same extent. The difference of *ca.* 6.8 kcal mol^{-1} with respect to the c_3 conformers could be ascribed to the favorable $LP_{O5} \rightarrow \sigma^*_{C3-S10}$ and $LP_{O5} \rightarrow \sigma^*_{C2-C3}$ orbital interactions for c_1 and c_2. It is noteworthy that the strong repulsive field effect between the $C^{\delta+}=O^{\delta-}$ and $C^{\delta+}-O^{\delta-}$ uniquely destabilize the c_1 conformer and increases its ν_{CO} frequency. Therefore, the order of stability of the three conformers

seemsto be reasonably determined by a balance between orbital and electrostatic interactions.

X-ray single crystal analysis of compound **6** reveals that in the solid state it assumes the least stable c_1 conformation found in vacuum. These molecules are stabilized through a series of intermolecular hydrogen bonds.

ACKNOWLEDGMENTS

The Brazilian authors thank the Fundação de Amparo à Pesquisa do Estado de São Paulo (FAPESP–2016/21676-0) for financial support of this research, the Conselho Nacional de Desenvolvimento Científico e Tecnológico (CNPq) for scholarships to D.N.S.R. and J.V. as well as fellowships to P.R.O. (301180/2013-0) and J.Z-S (303207/2017–5). This study was financed in part by the Coordenação de Aperfeiçoamento de Pessoal de Nível Superior – Brasil (CAPES) – Finance Code 001. The authors also thank Prof. Lucas C. Ducati and Patrick R. Batista for performing the NBO 6.0 calculations.

REFERENCES

[1] P. Chauhan, S. Mahajan, D. Enders, Organocatalytic Carbon–Sulfur Bond-Forming Reactions, Chem. Rev. 114 (2014) 8807–8864. doi:10.1021/cr500235v.

[2] R. Schulz, A. Atef, D. Becker, F. Gottschalk, C. Tauber, S. Wagner, C. Arkona, A.A. Abdel-Hafez, H.H. Farag, J. Rademann, G. Wolber, Phenylthiomethyl Ketone-Based Fragments Show Selective and Irreversible Inhibition of Enteroviral 3C Proteases, J. Med. Chem. 61 (2018) 1218–1230. doi:10.1021/acs.jmedchem.7b01440.

[3] E. Piras, F. Secci, P. Caboni, M.F. Casula, A. Frongia, α-Benzoyloxylation of β-keto sulfides at ambient temperature, RSC Adv. 7 (2017) 49215–49219. doi:10.1039/C7RA10888E.

[4] I. Paterson, V.A. Steadman neé Doughty, M.D. McLeod, T. Trieselmann, Stereocontrolled total synthesis of (+)-concanamycin F: the strategic use of boron-mediated aldol reactions of chiral ketones, Tetrahedron. 67 (2011) 10119–10128. doi:10.1016/j.tet.2011.09.012.

[5] C.R. Cerqueira, P.R. Olivato, M. Dal Colle, Conformational study of some 4′-substituted 2-(phenylselanyl)-2-(ethylsulfanyl)-acetophenones, Spectrochim.

Acta Part A Mol. Biomol. Spectrosc. 139 (2015) 495–504. doi:10.1016/j.saa.2014.12.077.

[6] C.R. Cerqueira, P.R. Olivato, D.N.S. Rodrigues, J. Zukerman-Schpector, E.R.T. Tiekink, M. Dal Colle, Stereochemical and electronic interaction studies of 4′-substituted 2-(phenylselanyl)-2-(ethylsulfinyl)-acetophenones, J. Mol. Struct. 1133 (2017) 49–65. doi:10.1016/j.molstruc.2016.11.077.

[7] C.R. Cerqueira, P.R. Olivato, D.N.S. Rodrigues, J. Zukerman-Schpector, E.R.T. Tiekink, M. Dal Colle, Conformational study of some 4′-substituted 2-(phenylselanyl)-2-(ethylsulfonyl)-acetophenones, J. Mol. Struct. 1084 (2015) 190–199. doi:10.1016/j.molstruc.2014.12.033.

[8] N. Baptistini, Analysis in silico, in vitro and in vivo of organochalcogens compounds as possible anti-inflamatories, Federal University of Sao Carlos, 2015. https://repositorio.ufscar.br/handle/ufscar/7554.

[9] I. Caracelli, J. Zukerman-Schpector, H.J. Traesel, P.R. Olivato, M.M. Jotani, E.R.T. Tiekink, 2-[(4-Chlorophenyl)sulfanyl]-2-methoxy-1-phenylethan-1-one: crystal structure and Hirshfeld surface analysis, Acta Crystallogr. Sect. E Crystallogr. Commun. 74 (2018) 703–708. doi:10.1107/S2056989018006072.

[10] J. Zukerman-Schpector, P.R. Olivato, H.J. Traesel, J. Valença, D.N.S. Rodrigues, E.R.T. Tiekink, Crystal structure of 2-methoxy-2-[(4-methylphenyl)sulfanyl]-1-phenylethan-1-one, Acta Crystallogr. Sect. E Crystallogr. Commun. 71 (2015) o3–o4. doi:10.1107/S205698901402550X.

[11] I. Caracelli, P.R. Olivato, H.J. Traesel, J. Valença, D.N.S. Rodrigues, E.R.T. Tiekink, Crystal structure of 2-methoxy-2-[(4-methoxyphenyl)sulfanyl]-1-phenylethanone, Acta Crystallogr. Sect. E Crystallogr. Commun. 71 (2015) o657–o658. doi:10.1107/S2056989015014565.

[12] P.R. Olivato, R. Rittner, Conformational and electronic interaction studies of some alpha-mono-heterosubstituted carbonyl compounds, Rev. Heteroat. Chem. 15 (1996) 115–159.

[13] E. Vinhato, P.R. Olivato, J. Zukerman-Schpector, M. Dal Colle, Conformational analysis of some N,N-diethyl-2-[(4′-substituted) phenylthio] acetamides, Spectrochim. Acta Part A Mol. Biomol. Spectrosc. 115 (2013) 738–746. doi:10.1016/j.saa.2013.06.118.

[14] P.R. Olivato, N.L.C. Domingues, M.G. Mondino, C.F. Tormena, R. Rittner, M. Dal Colle, Spectroscopic and theoretical studies of some N-methoxy-N-methyl-2-

[(4′-substituted) phenylthio]propanamides, J. Mol. Struct. 920 (2009) 393–400. doi:10.1016/j.molstruc.2008.11.040.

[15] P. Olivato, J. Santos, B. Contieri, C. Cerqueira, D. Rodrigues, E. Vinhato, J. Zukerman-Schpector, M. Colle, Spectroscopic and Theoretical Studies of Some 3-(4′-Substituted phenylsulfanyl)-1-methyl-2-piperidones, Molecules. 18 (2013) 7492–7509. doi:10.3390/molecules18077492.

[16] S.A. Guerrero, P.R. Olivato, R. Rittner, A conformational analysis of some α-aryloxy p-substituted-acetophenones: Solvent effects on the νCO infrared bands, Can. J. Anal. Sci. Spectrosc. 48 (2003) 181–188.

[17] S. Cradock, R.A. Whiteford, Photoelectron spectra of the methyl, silyl and germyl derivatives of the group VI elements, J. Chem. Soc. Faraday Trans. 2. 68 (1972) 281–288. doi:10.1039/f29726800281.

[18] C. Dezarnaud, M. Tronc, A. Modelli, Shape resonances in low-energy electron transmission and sulfur K-shell photoabsorption spectroscopies: CH3SH, C2H5SH, (CH3)2S, (C2H5)2S, C6H5SH, C6H5SCH3, CH3SCN, CH3NCS, SCl2, Chem. Phys. 156 (1991) 129–140. doi:10.1016/0301-0104(91)87045-W.

[19] J.C. Giordan, J.H. Moore, J.A. Tossell, W. Kaim, Interaction of frontier orbitals of Group 15 and Group 16 methides with the frontier orbitals of benzene, J. Am. Chem. Soc. 107 (1985) 5600–5604. doi:10.1021/ja00306a003.

[20] A. Modelli, D. Jones, G. Distefano, M. Tronc, Electron affinity and dissociative electron attachment in saturated dialkyl group-16 derivatives, Chem. Phys. Lett. 181 (1991) 361–366. doi:10.1016/0009-2614(91)80085-C.

[21] Refers to the electron-affinity of the diethyl ether.

[22] H.J. Traesel, P.R. Olivato, J. Valença, D.N.S. Rodrigues, J. Zukerman-Schpector, M.D. Colle, Conformational analysis of some 4′-substituted 2-(phenylselanyl)- 2-(methoxy)- acetophenones, J. Mol. Struct. 1157 (2018) 29–39. doi:10.1016/j.molstruc.2017.12.040.

[23] P.A. Zoretic, P. Soja, Sulfenylation and selenenylation of lactams, J. Org. Chem. 41 (1976) 3587–3589. doi:10.1021/jo00884a022.

[24] F.E. Romesberg, M.P. Bernstein, J.H. Gilchrist, A.T. Harrison, D.J. Fuller, D.B. Collum, Structure of lithium hexamethyldisilazide in the presence of hexamethylphosphoramide. Spectroscopic and computational studies of monomers, dimers, and triple ions, J. Am. Chem. Soc. 115 (1993) 3475–3483. doi:10.1021/ja00062a010.

[25] H.J. Reich, W.H. Sikorski, Regioselectivity of Addition of Organolithium Reagents to Enones: The Role of HMPA, J. Org. Chem. 64 (1999) 14–15. doi:10.1021/jo981765g.

[26] C.L. Angell, P.J. Krueger, R. Lauzon, L.C. Leitch, K. Noack, R.J.D. Smith, R.N. Jones, The carbonyl stretching frequency of cyclopentanone, Spectrochim. Acta. 15 (1959) 926–931. doi:10.1016/S0371-1951(59)80390-8.

[27] Galactic Industries Corporation, 1991-1998, Salem, USA.

[28] N.B. Colthup, L.H. Daly, S.E. Wiberley, Introduction to Infrared and Raman Spectroscopy, in: Introd. to Infrared Raman Spectrosc., THIRD EDIT, Elsevier, USA, 1990. doi:10.1016/B978-0-08-091740-5.50001-6.

[29] G.M. Sheldrick. SADABS, Program for Empirical Absorption Correction of Area Detector Data; University of Göttingen: Germany, 1996.

[30] Bruker. APEX2 and SAINT; Bruker AXS Inc.: Madison, WI, USA, 2007.

[31] M.C. Burla, R. Caliandro, B. Carrozzini, G.L. Cascarano, C. Cuocci, C. Giacovazzo, M. Mallamo, A. Mazzone, G. Polidori, Crystal structure determination and refinement via SIR2014, J. Appl. Crystallogr. 48 (2015) 306–309. doi:10.1107/S1600576715001132.

[32] G.M. Sheldrick, Crystal structure refinement with SHELXL, Acta Crystallogr. Sect. C Struct. Chem. 71 (2015) 3–8. doi:10.1107/S2053229614024218.

[33] L.J. Farrugia, WinGX and ORTEP for Windows : an update, J. Appl. Crystallogr. 45 (2012) 849–854. doi:10.1107/S0021889812029111.

[34] Y. Shao, L.F. Molnar, Y. Jung, J. Kussmann, C. Ochsenfeld, S.T. Brown, A.T.B. Gilbert, L. V. Slipchenko, S. V. Levchenko, D.P. O'Neill, R.A. DiStasio Jr, R.C. Lochan, T. Wang, G.J.O. Beran, N.A. Besley, J.M. Herbert, C. Yeh Lin, T. Van Voorhis, S. Hung Chien, A. Sodt, R.P. Steele, V.A. Rassolov, P.E. Maslen, P.P. Korambath, R.D. Adamson, B. Austin, J. Baker, E.F.C. Byrd, H. Dachsel, R.J. Doerksen, A. Dreuw, B.D. Dunietz, A.D. Dutoi, T.R. Furlani, S.R. Gwaltney, A. Heyden, S. Hirata, C.-P. Hsu, G. Kedziora, R.Z. Khalliulin, P. Klunzinger, A.M. Lee, M.S. Lee, W. Liang, I. Lotan, N. Nair, B. Peters, E.I. Proynov, P.A. Pieniazek, Y. Min Rhee, J. Ritchie, E. Rosta, C. David Sherrill, A.C. Simmonett, J.E. Subotnik, H. Lee Woodcock III, W. Zhang, A.T. Bell, A.K. Chakraborty, D.M. Chipman, F.J. Keil, A. Warshel, W.J. Hehre, H.F. Schaefer III, J. Kong, A.I. Krylov, P.M.W. Gill, M. Head-Gordon, Advances in methods and algorithms in a modern quantum chemistry program package, Phys. Chem.

Chem. Phys. 8 (2006) 3172–3191. doi:10.1039/B517914A.

[35] M.J. Frisch, G.W. Trucks, H.B. Schlegel, G.E. Scuseria, M.A. Robb, J.R. Cheeseman, G. Scalmani, V. Barone, B. Mennucci, G.A. Petersson, H. Nakatsuji, M. Caricato, X. Li, H.P. Hratchian, A.F. Izmaylov, J. Bloino, G. Zheng, J.L. Sonnenberg, M. Hada, M. Ehara, K. Toyota, R. Fukuda, J. Hasegawa, M. Ishida, T. Nakajima, Y. Honda, O. Kitao, H. Nakai, T. Vreven, J.A. Montgomery Jr., J.E. Peralta, F. Ogliaro, M. Bearpark, J.J. Heyd, E. Brothers, K.N. Kudin, V.N. Staroverov, R. Kobayashi, J. Normand, K. Raghavachari, A. Rendell, J.C. Burant, S.S. Iyengar, J. Tomasi, M. Cossi, N. Rega, J.M. Millam, M. Klene, J.E. Knox, J.B. Cross, V. Bakken, C. Adamo, J. Jaramillo, R. Gomperts, R.E. Stratmann, O. Yazyev, A.J. Austin, R. Cammi, C. Pomelli, J.W. Ochterski, R.L. Martin, K. Morokuma, V.G. Zakrzewski, G.A. Voth, P. Salvador, J.J. Dannenberg, S. Dapprich, A.D. Daniels, Ö. Farkas, J.B. Foresman, J.V. Ortiz, J. Cioslowski, D.J. Fox, Gaussian 09 Revision D.01, Gaussian Inc., Wallingford CT, 2013.

[36] A.D. Becke, Density- functional thermochemistry. III. The role of exact exchange, J. Chem. Phys. 98 (1993) 5648–5652. doi:10.1063/1.464913.

[37] A.D. Becke, A new mixing of Hartree–Fock and local density- functional theories, J. Chem. Phys. 98 (1993) 1372–1377. doi:10.1063/1.464304.

[38] C. Lee, W. Yang, R.G. Parr, Development of the Colle-Salvetti correlation-energy formula into a functional of the electron density, Phys. Rev. B. 37 (1988) 785–789. doi:10.1103/PhysRevB.37.785.

[39] M. Cossi, G. Scalmani, N. Rega, V. Barone, New developments in the polarizable continuum model for quantum mechanical and classical calculations on molecules in solution, J. Chem. Phys. 117 (2002) 43–54. doi:10.1063/1.1480445.

[40] J. Tomasi, B. Mennucci, R. Cammi, Quantum Mechanical Continuum Solvation Models, Chem. Rev. 105 (2005) 2999–3094. doi:10.1021/cr9904009.

[41] E.D. Glendening, J.K. Badenhoop, A.E. Reed, J.E. Carpenter, J.A. Bohmann, C.M. Morales, C.R. Landis, F. Weinhold, NBO Version 6.0.

[42] C.M. Breneman, K.B. Wiberg, Determining atom-centered monopoles from molecular electrostatic potentials. The need for high sampling density in formamide conformational analysis, J. Comput. Chem. 11 (1990) 361–373. doi:10.1002/jcc.540110311.

[43] Y. Zhao, D.G. Truhlar, Density Functionals with Broad Applicability in Chemistry, Acc. Chem. Res. 41 (2008) 157–167. doi:10.1021/ar700111a.

[44] S. Grimme, J. Antony, S. Ehrlich, H. Krieg, A consistent and accurate ab initio parametrization of density functional dispersion correction (DFT-D) for the 94 elements H-Pu, J. Chem. Phys. 132 (2010) 154104. doi:10.1063/1.3382344.

[45] M.J. Frisch, G.W. Trucks, H.B. Schlegel, G.E. Scuseria, M.A. Robb, J.R. Cheeseman, G. Scalmani, V. Barone, B. Mennucci, G.A. Petersson, H. Nakatsuji, M. Caricato, X. Li, H.P. Hratchian, A.F. Izmaylov, J. Bloino, G. Zheng, J.L. Sonnenberg, M. Hada, M. Ehara, K. Toyota, R. Fukuda, J. Hasegawa, M. Ishida, T. Nakajima, Y. Honda, O. Kitao, H. Nakai, T. Vreven, J.A. Montgomery Jr., J.E. Peralta, F. Ogliaro, M. Bearpark, J.J. Heyd, E. Brothers, K.N. Kudin, V.N. Staroverov, R. Kobayashi, J. Normand, K. Raghavachari, A. Rendell, J.C. Burant, S.S. Iyengar, J. Tomasi, M. Cossi, N. Rega, J.M. Millam, M. Klene, J.E. Knox, J.B. Cross, V. Bakken, C. Adamo, J. Jaramillo, R. Gomperts, R.E. Stratmann, O. Yazyev, A.J. Austin, R. Cammi, C. Pomelli, J.W. Ochterski, R.L. Martin, K. Morokuma, V.G. Zakrzewski, G.A. Voth, P. Salvador, J.J. Dannenberg, S. Dapprich, A.D. Daniels, Ö. Farkas, J.B. Foresman, J.V. Ortiz, J. Cioslowski, D.J. Fox, Gaussian 09 Revision A.02, Gaussian Inc., Wallingford CT, 2009.

[46] M.H. Jamróz, Vibrational Energy Distribution Analysis (VEDA): Scopes and limitations, Spectrochim. Acta Part A Mol. Biomol. Spectrosc. 114 (2013) 220–230. doi:10.1016/j.saa.2013.05.096.

[47] D.R. Lide, Ed. CRC Handbook of Chemistry and Physics, CRC Press, Boca Raton, FL, 2005.

[48] A. Gaset, L. Lafaille, A. Verdier, A. Lattes, Infrared spectra of α-aminoketones; configurational study and evidence of an enol form, Bull. Soc. Chim. Fr. 10 (1968) 4108–4112.

[49] L.J. Bellamy, Advances in infrared Group Frequencies, in: Chapman and Hall, London, 1975: pp. 141–142.

[50] J.F. Bertran, L. Ballester, L. Dobrihalova, N. Sánchez, R. Arrieta, Study of Fermi resonance by the method of solvent variation, Spectrochim. Acta Part A Mol. Spectrosc. 24 (1968) 1765–1776. doi:10.1016/0584-8539(68)80232-6.

[51] R. Cataliotti, R.N. Jones, Further evidence of Fermi resonance in the C-O stretching band of cyclopentanone, Spectrochim. Acta Part A Mol. Spectrosc. 27

(1971) 2011–2013. doi:10.1016/0584-8539(71)80254-4.

[52] J. Overend, Quantitative intensity studies and dipole moment derivatives, in: Infrared Spectroscopy and Molecular structure, M. Davis Ed., Chapter 10, p 352, Elsevier, New York, 1963.

[53] R.A. Nyquist, Solvent-Induced Carbonyl Frequency Shifts: Cyclopentanone and Cyclohexanone, Appl. Spectrosc. 44 (1990) 426–433. doi:10.1366/0003702904086290.

[54] X.-L. Jiang, D.-F. Li, C.-L. Sun, Z.-L. Li, G. Yang, M. Zhou, Z.-W. Li, S.-Q. Gao, Relationship between Fermi Resonance and Solvent Effects, Chinese Phys. Lett. 28 (2011) 053301-1-053301-4. doi:10.1088/0256-307X/28/5/053301.

[55] C.C. Levin, R. Hoffmann, W.J. Hehre, J. Hudec, Orbital interaction in amino-ketones, J. Chem. Soc. Perkin Trans. 2. 2 (1973) 210–220. doi:10.1039/p29730000210.

[56] S. David, O. Eisenstein, W.J. Hehre, L. Salem, R. Hoffmann, Superjacent orbital control. Interpretation of the anomeric effect, J. Am. Chem. Soc. 95 (1973) 3806–3807. doi:10.1021/ja00792a062.

Figure and Scheme Captions

Scheme 1. Atoms labelling of 2-(methoxy)-2-[(4-substituded)-phenylsulfanyl]-[(4'-substituted)-acetophenones] (**1**-**7**), the corresponding methyne deuterated compounds (**1a**-**5a**), and definition of relevant dihedral angles.

Scheme 2. Bar diagram showing the experimental highest and medium ν_{CO} stretching frequency components ($\nu_{n/m}$, cm^{-1}) and the calculated unperturbed frequencies ($\nu^0_{n/m}$, cm^{-1}) of compound **4**, along with the higher doublet frequency component [$\nu_{CO(C\text{-}D)}$, cm^{-1}] of the corresponding methyne deuterated compound (**4a**). The relative intensities and the frequencies of the carbonyl band components were drawn to match the experimental values.

Figure 1. IR spectra of 2-(phenylsulfanyl)-2-(methoxy)-acetophenone **3**, showing the analytically resolved carbonyl stretching band, in: *n*-hexane (**a**), carbon tetrachloride [fundamental (**b**) and first overtone (**c**)], chloroform (**d**), dichloromethane (**e**) and acetonitrile (**f**).

Figure 2. IR spectra of 2-(deutero)-2-(phenylsulfanyl)-2-(methoxy)-acetophenone **3a**, showing the analytically resolved carbonyl stretching band, in: *n*-hexane (**a**), carbon tetrachloride [fundamental (**b**) and first overtone (**c**)], chloroform (**d**), dichloromethane (**e**) and acetonitrile (**f**).

Figure 3. IR spectra of 2-(phenylsulfanyl)-2-(methoxy)-4'-methoxy-acetophenone **6**, showing the analytically resolved carbonyl stretching band, in: *n*-hexane (**a**), carbon tetrachloride [fundamental (**b**) and first overtone (**c**)], chloroform (**d**), dichloromethane (**e**) and acetonitrile (**f**).

Figure 4. Molecular structures of the conformers of **3** obtained at the B3LYP/6-31+G(d,p) level. Adopted colors: H = white, C = grey, O = red, S = yellow.

Figure 5. ORTEP view of the asymmetric unit of **6** showing atom labelling and displacement ellipsoids at the 40% probability level.

Figure 6. ORTEP view of **6** showing the molecules held through C-H…O interactions, and displacement ellipsoids at the 40% probability level.

Supplementary Figures and Scheme Captions

Figure S1. IR spectra of 2-(4-methoxy-phenylsulfanyl)-2-(methoxy)-acetophenone **1**, showing the analytically resolved carbonyl stretching band, in: carbon tetrachloride [fundamental (**a**) and first overtone (**b**)], chloroform (**c**), dichloromethane (**d**) and acetonitrile (**e**).

Figure S2. IR spectra of 2-(4-methyl-phenylsulfanyl)-2-(methoxy)-acetophenone **2**, showing the analytically resolved carbonyl stretching band, in: *n*-hexane (**a**), carbon tetrachloride [fundamental (**b**) and first overtone (**c**)], chloroform (**d**), dichloromethane (**e**) and acetonitrile (**f**).

Figure S3. IR spectra of 2-(4-chloro-phenylsulfanyl)-2-(methoxy)-acetophenone **4**, showing the analytically resolved carbonyl stretching band, in: carbon tetrachloride

[fundamental (**a**) and first overtone (**b**)], chloroform (**c**), dichloromethane (**d**) and acetonitrile (**e**).

Figure S4. IR spectra of 2-(4-bromo-phenylsulfanyl)-2-(methoxy)-acetophenone **5**, showing the analytically resolved carbonyl stretching band, in: carbon tetrachloride [fundamental (**a**) and first overtone (**b**)], chloroform (**c**), dichloromethane (**d**) and acetonitrile (**e**).

Figure S5. IR spectra of 2-(deutero)-2-(4-methoxy-phenylsulfanyl)-2-(methoxy)-acetophenone **1a**, showing the analytically resolved carbonyl stretching band, in: carbon tetrachloride [fundamental (**a**) and first overtone (**b**)], chloroform (**c**), dichloromethane (**d**) and acetonitrile (**e**).

Figure S6. IR spectra of 2-(deutero)-2-(4-methyl-phenylsulfanyl)-2-(methoxy)-acetophenone **2a**, showing the analytically resolved carbonyl stretching band, in: *n*-hexane (**a**), carbon tetrachloride [fundamental (**b**) and first overtone (**c**)], chloroform (**d**), dichloromethane (**e**) and acetonitrile (**f**).

Figure S7. IR spectra of 2-(deutero)-2-(4-chloro-phenylsulfanyl)-2-(methoxy)-acetophenone **4a**, showing the analytically resolved carbonyl stretching band, in: carbon tetrachloride [fundamental (**a**) and first overtone (**b**)], chloroform (**c**), dichloromethane (**d**) and acetonitrile (**e**).

Figure S8. IR spectra of 2-(deutero)-2-(4-bromo-phenylsulfanyl)-2-(methoxy)-acetophenone **5a**, showing the analytically resolved carbonyl stretching band, in: carbon tetrachloride [fundamental (**a**) and first overtone (**b**)], chloroform (**c**), dichloromethane (**d**) and acetonitrile (**e**).

Figure S9. IR spectra of 2-(phenylsulfanyl)-2-(methoxy)-4'-chloro-acetophenone **7**, showing the analytically resolved carbonyl stretching band, in: n-hexane (**a**), carbon tetrachloride [fundamental (**b**) and first overtone (**c**)], chloroform (**d**), dichloromethane (**e**) and acetonitrile (**f**).

Scheme S1. Bar diagrams showing the experimental highest and medium ν_{CO} stretching frequency components ($\nu_{n/m}$, cm^{-1}) and the calculated unperturbed frequencies ($\nu^0_{n/m}$, cm^{-1}) for compounds **1**-**3** and **5**. The relative intensities and the frequencies of the carbonyl band components were drawn to match the experimental values.

Figure 1

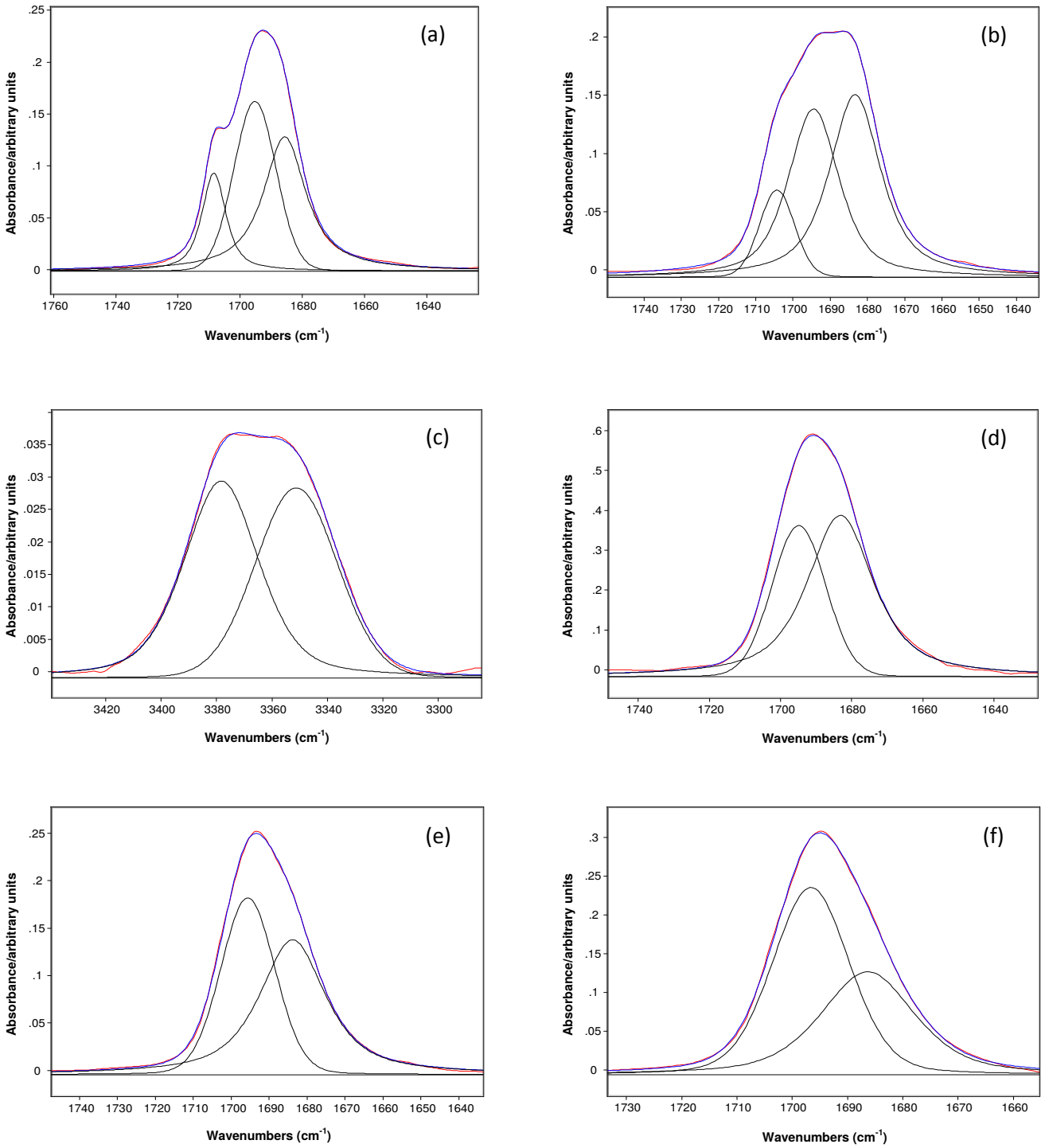

Figure 1. IR spectra of 2-(phenylsulfanyl)-2-(methoxy)-acetophenone **3**,showing the analytically resolved carbonyl stretching band, in: *n*-hexane (**a**), carbon tetrachloride [fundamental (**b**) and first overtone (**c**)], chloroform (**d**), dichloromethane (**e**) and acetonitrile (**f**).

Figure 2

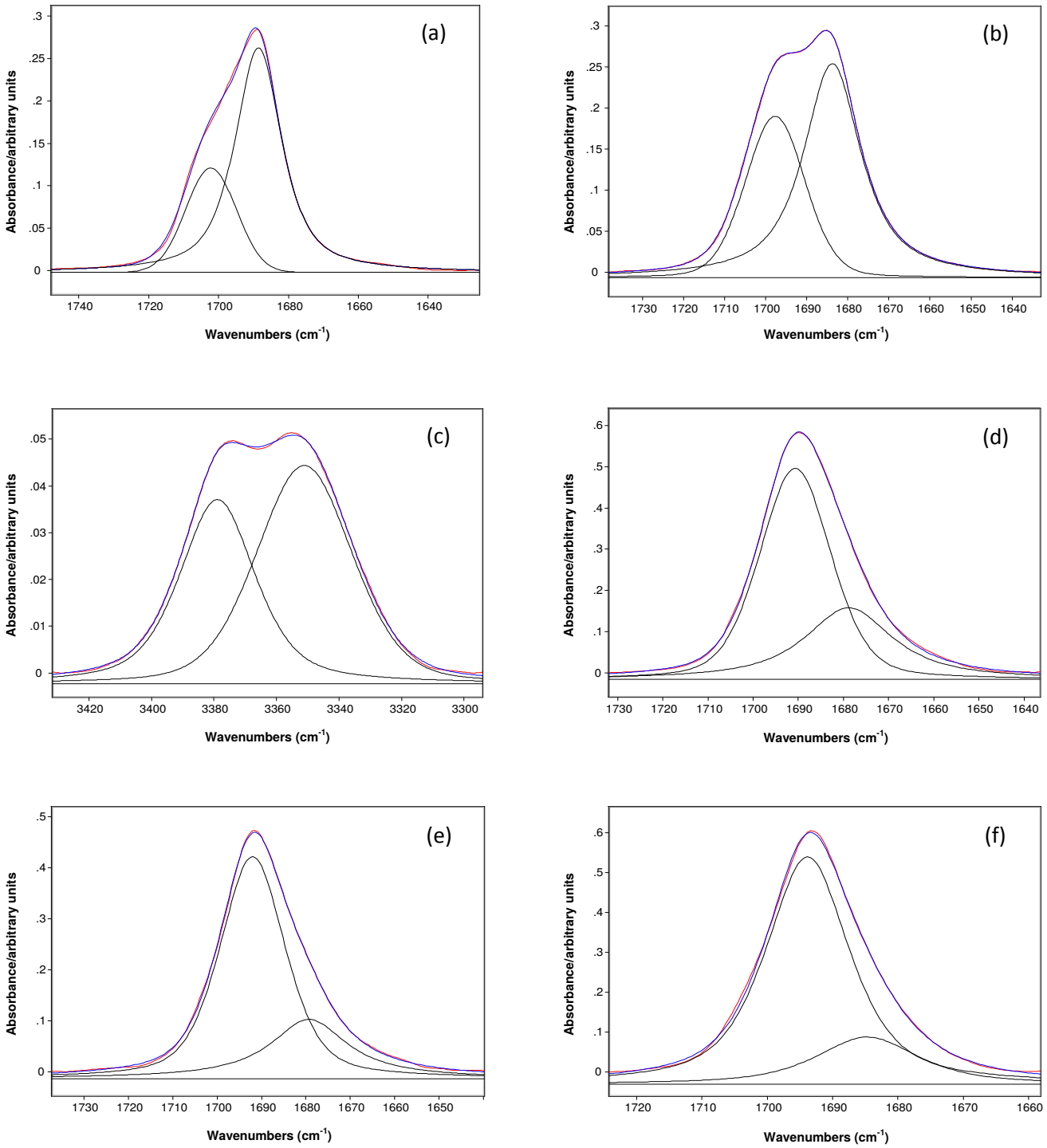

Figure 2. IR spectra of 2-(deutero)-2-(phenylsulfanyl)-2-(methoxy)-acetophenone **3a**,showing the analytically resolved carbonyl stretching band, in: *n*-hexane (**a**), carbon tetrachloride [fundamental (**b**) and first overtone (**c**)], chloroform (**d**), dichloromethane (**e**) and acetonitrile (**f**).

Figure 3

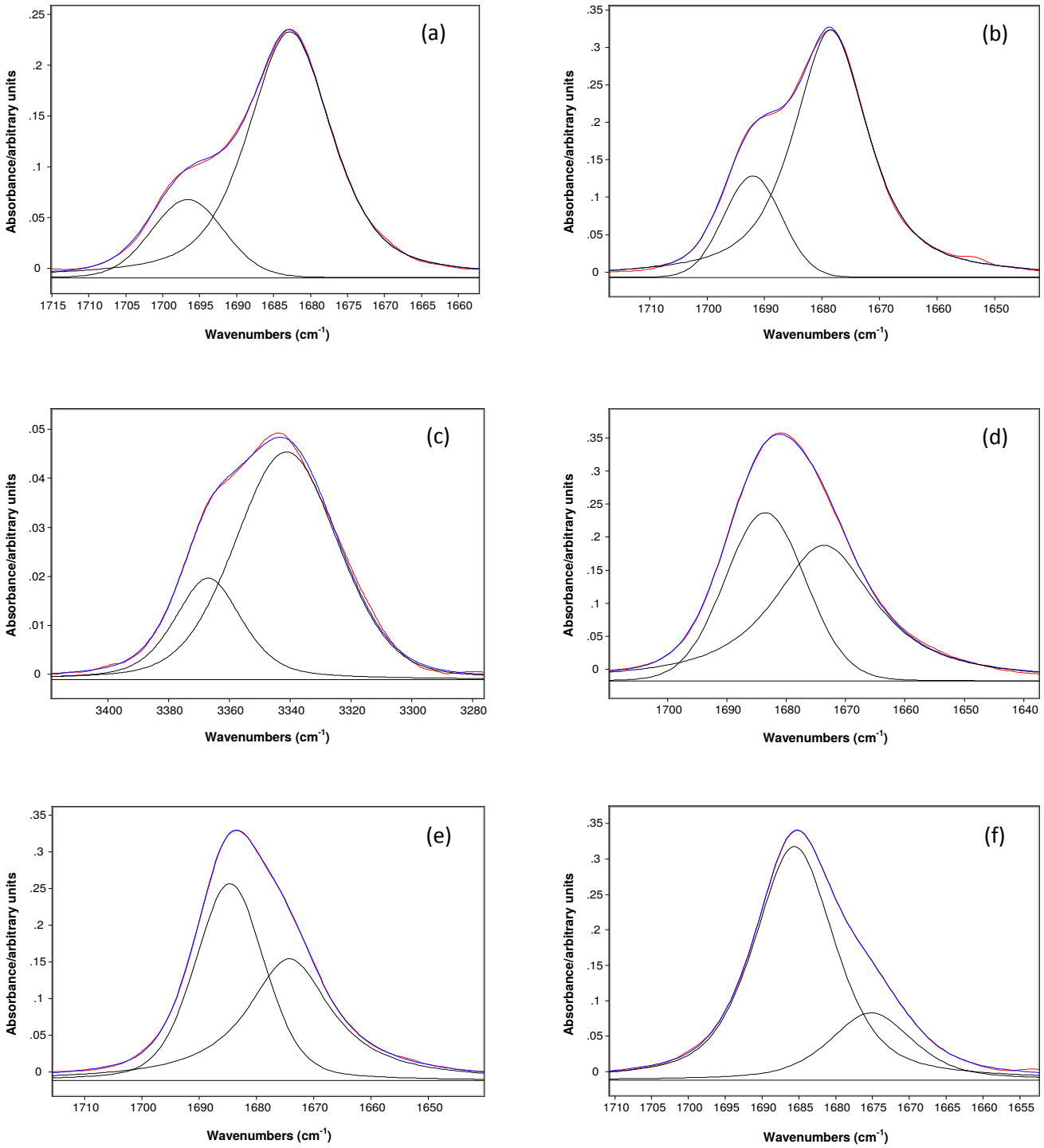

Figure 3. IR spectra of 2-(phenylsulfanyl)-2-(methoxy)-4'-methoxy-acetophenone **6**,showing the analytically resolved carbonyl stretching band, in: *n*-hexane (**a**), carbon tetrachloride [fundamental (**b**) and first overtone (**c**)], chloroform (**d**), dichloromethane (**e**) and acetonitrile (**f**).

Figure 4

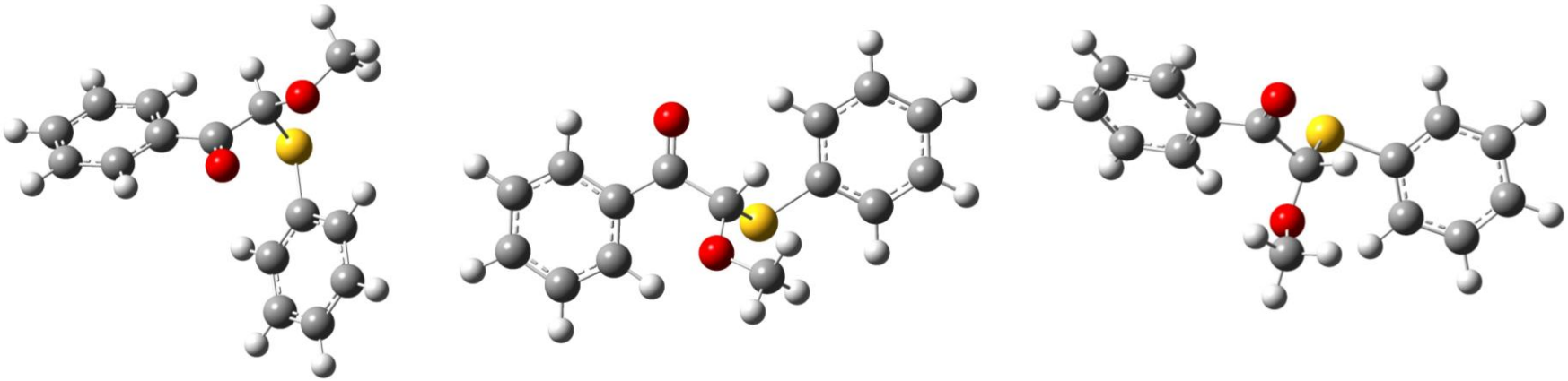

c_1 c_2 c_3

Figure 4. Molecular structures of the conformers of **3** obtained at the B3LYP/6-31+G(d,p)level. Adopted colors: H = white, C = grey, O = red, S = yellow.

Figure 5

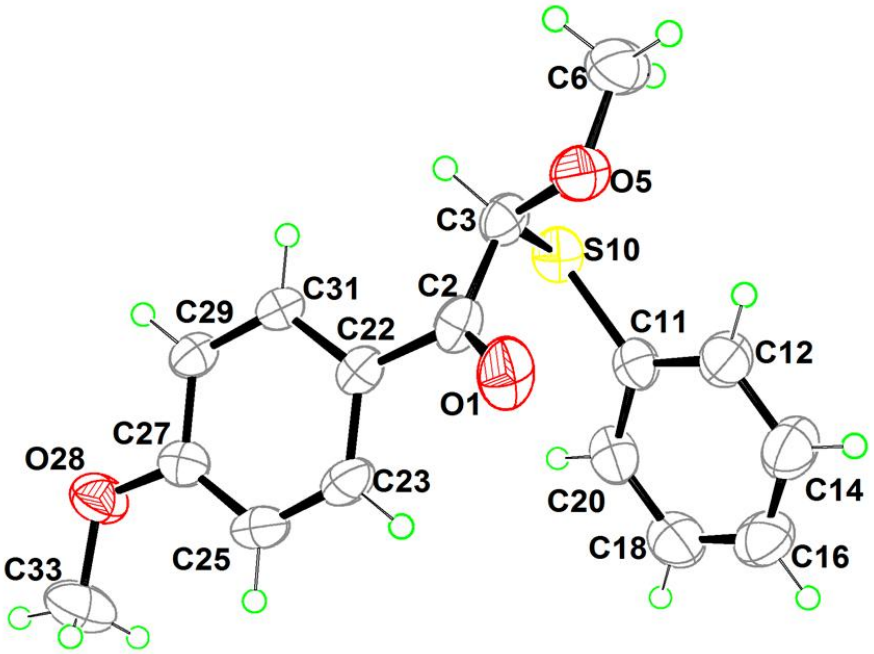

Figure 5. ORTEP view of the asymmetric unit of **6** showing atom labelling and displacement ellipsoids at the 40% probability level.

Figure 6

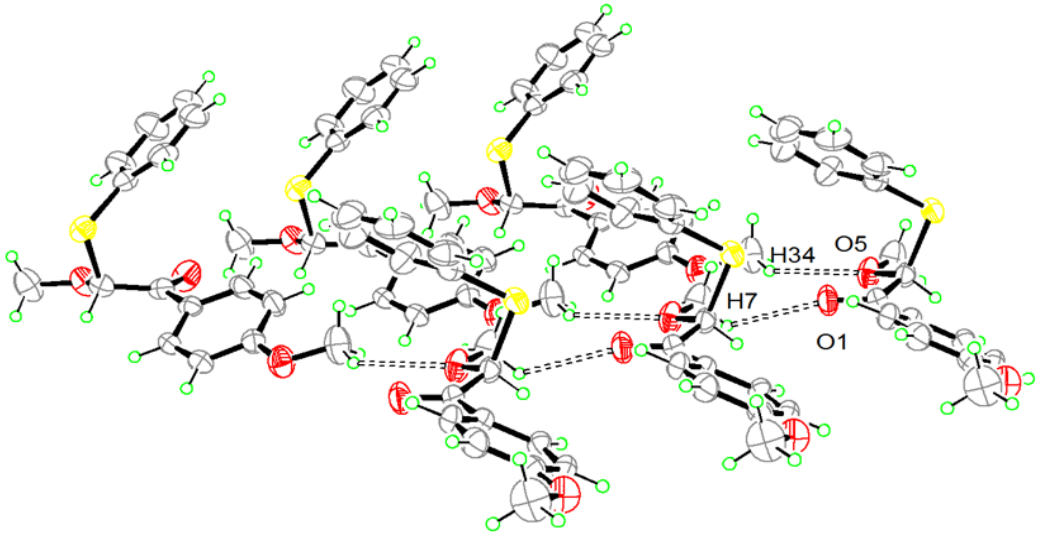

Figure 6.ORTEP view of **6** showing the molecules held through C-H…O interactions, and displacement ellipsoids at the 40% probability level.

Scheme 1

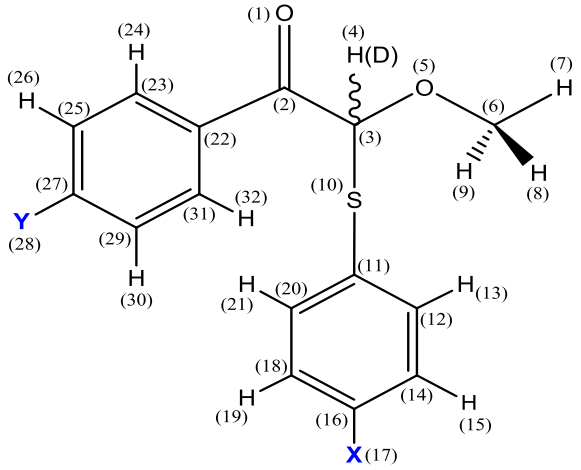

For 4'-**Y** = OMe (**6**), Cl (**7**)

4-**X** = H

α = O(1)-C(2)-C(3)-O(5)

β = C(2)-C(3)-O(5)-C(6)

δ = O(1)-O(2)-C(22)-C(23)

ϕ = O(5)-C(3)-S(10)-C(11)

For 4-**X** = OMe (**1**), Me (**2**), H (**3**), Cl (**4**), Br (**5**)

4'-**Y** = H

α' = O(1)-C(2)-C(3)-S(10)

β' = C(2)-C(3)-S(10)-C(11)

γ' = C(3)-S(10)-C(11)-C(12)

ϕ' = S(10)-C(3)-O(5)-C(6)

Scheme 1. Atoms labelling of 2-(methoxy)-2-[(4-substituded)-phenylsulfanyl]-[(4'-substituted)-acetophenones] (**1**-**7**), the corresponding methyne deuterated compounds (**1a**-**5a**), and definition of relevant dihedral angles.

Scheme 2

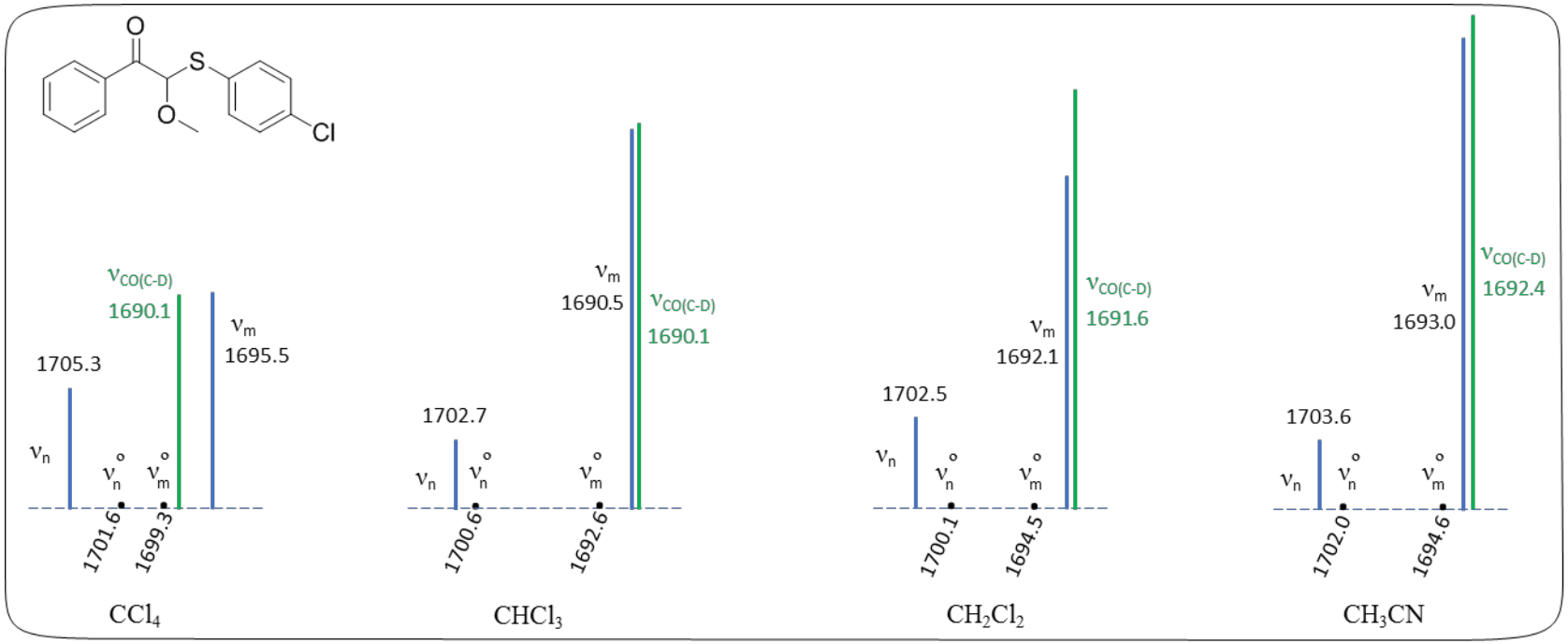

Scheme 2. Bar diagram showing the experimental highest and medium ν_{CO} stretching frequency components ($\nu_{n/m}$, cm^{-1}) and the calculated unperturbed frequencies ($\nu^0_{n/m}$, cm^{-1}) of compound **4**, along with the higher doublet frequency component [$\nu_{CO(C-D)}$, cm^{-1}] of the corresponding methyne deuterated compound (**4a**). The relative intensities and the frequencies of the carbonyl band components were drawn to match the experimental values.

Table 1

^{1}H, ^{13}C NMR and elemental analysis data for 4- and 4'-substituted 2-(methoxy)-2-(phenylsulfanyl)-acetophenones 4'-Y-PhC(O)CH[OMe][SPh-4-X] (**1**-**7**)

Comp.	Y	X	^{1}H NMR[a]	^{13}C NMR[a]	Mp (°C)	Molecular formula	Elemental Analysis / %		
								C	H
1	H	OCH_3	7.95-7.94 (2H, m), 7.57 (1H, m), 7.46-7.44 (2H, m), 7.26-7.24 (2H, m), 6.81-6.80 (2H, m), 5.76 (1H, s), 3.78 (3H, s), 3.68 (3H, s)	190.26, 160.49, 136.75, 134.53, 133.28, 128.84, 128.49, 120.83, 114.64, 89.79, 56.16, 55.28	120.5-121.2	$C_{16}H_{16}O_3S$	Calc. Found	66.64 66.52	5.59 5.53
2	H	CH_3	7.97-7.95 (2H, m), 7.57 (1H, m), 7.46-7.44 (2H, m), 7.25-7.24 (2H, m), 7.10-7.08 (2H, m), 5.81 (1H, s), 3.67 (3H, s), 2.33 (3H, s)	190.55, 139.07, 134.60, 134.44, 133.32, 129.86, 128.91, 128.49, 127.25, 90.01, 56.13, 21.25	86.3-86.8	$C_{16}H_{16}O_2S$	Calc. Found	70.56 69.96	5.92 6.02
3	H	H	7.97-7.95 (2H, m), 7.58 (1H, m), 7.46-7.43 (2H, m), 7.39-7.37 (2H, m), 7.32-7.28 (3H, m), 5.86 (1H, s), 3.68 (3H, s)	190.65, 134.34, 134.19, 133.40, 131.23, 129.04, 128.93, 128.72, 128.50, 90.07, 56.10	54.8-55.3	$C_{15}H_{14}O_2S$	Calc. Found	69.74 69.74	5.46 5.72
4	H	Cl	7.95-7.93 (2H, m), 7.59 (1H, m), 7.47-7.44 (2H, m), 7.29-7.24 (4H, m), 5.86 (1H, s), 3.67 (3H, s)	190.20, 135.60, 135.25, 134.23, 133.55, 129.22, 128.84, 128.59, 89.37, 56.13	85.5-85.8	$C_{15}H_{13}ClO_2S$	Calc. Found	61.53 61.47	4.48 4.55
5	H	Br	7.94-7.92 (2H, m), 7.58 (1H, m), 7.47-7.44 (2H, m), 7.41-7.39 (2H, m), 7.22-7.20 (2H, m), 5.87 (1H, s), 3.67 (3H, s)	190.16, 135.73, 134.18, 133.53, 132.13, 129.92, 128.81, 128.57, 123.41, 89.28, 56.10	84.0-84.5	$C_{15}H_{13}BrO_2S$	Calc. Found	53.42 53.19	3.89 3.85
6	OCH_3	H	7.98-7.97 (2H, m), 7.41-7.39 (2H, m), 7.31-7.28 (3H, m), 6.93-6.91 (2H, m), 5.81 (1H, s), 3.87 (3H, s), 3.64 (3H, s)	189.63, 163.77, 133.98, 131.77, 131.43, 129.02, 128.55, 127.00, 113.73, 90.55, 56.01, 55.50	70.3-70.8	$C_{16}H_{16}O_3S$	Calc. Found	66.64 66.60	5.59 5.57
7	Cl	H	7.91-7.87 (2H, m), 7.42-7.40 (2H, m), 7.37-7.36 (2H, m), 7.32-7.28 (3H, m), 5.77 (1H, s), 3.67 (3H, s)	189.57, 139.83, 134.22, 132.55, 130.95, 130.43, 129.10, 128.86, 128.81, 90.39, 56.21	64.4-64.9	$C_{15}H_{13}ClO_2S$	Calc. Found	61.53 61.07	4.48 4.49

[a] ^{1}H and ^{13}C chemical shifts in ppm relative to TMS, in $CDCl_3$.

Table 2
Crystal data and structure refinement for **6**

Chemical formula	$C_{16}H_{16}O_3S$
Formula mass (g mol^{-1})	288.35
T (K)	293
Crystal system	Monoclinic
Space group	$P2_1/c$
Unit cell dimensions	
a (Å)	10.9628(4)
b (Å)	6.0281(2)
c (Å)	22.0394(7)
α(◦)	90
β(◦)	94.358(1)
γ(◦)	90
Volume ($Å^3$)	1452.26(9)
Z	4
D_{calc} (g/cm^3)	1.319
F(000)	608
μ (Mo $K\alpha$)/mm^{-1}	0.227
θ_{max} (°)	26.4
Measured data	18360
Unique data	2992
Observed data ($I \geq 2.0\sigma(I)$)	2627
R, obs. data; all data	0.0370; 0.0423
a, b in weighting scheme	0.0545, 0.3736
R_w, obs. data; all data	0.1036; 0.1087

Table 3

Experimental frequencies (ν, cm^{-1}) and intensities of the carbonyl stretching bands in the IR spectra of 4 and 4'-substituted 2-(methoxy)-2-(phenylsulfanyl)-acetophenones 4'-Y-PhC(O)CH[OMe][SPh-4-X] (**1-7**) in solvents of increasing relative permittivity

Comp.	Y	X	*n*-C_6H_{14} (ε = 1.9)		CCl_4 (ε = 2.2)				$CHCl_3$ (ε = 4.8)		CH_2Cl_2 (ε = 9.1)		CH_3CN (ε = 38)	
			ν	P[b]	ν	P	2ν[c]	P	ν	P	ν	P	ν	P
1	H	OMe	-[a]	-	1705	14.5	-	-[d]	-[d]	-[d]	1703	7.1	-[d]	-[d]
			-	-	1695	45.1	3377	59.5	1691	68.0	1691	78.9	1693	90.0
			-	-	1680	40.4	3346	40.5	1682	32.0	1675	14.0	1684	10.0
2	H	Me	1708	25.3	1705	22.0	-	-[d]	-[d]	-[d]	-	-	-[d]	-[d]
			1698	27.5	1696	32.6	3378	53.1	1694	41.8	1692	85.2	1695	64.8
			1688	47.2	1683	45.4	3349	46.9	1685	58.2	1676	14.8	1689	35.2
3	H	H	1708	24.4	1704	19.9	-	-[d]	-[d]	-[d]	-	-	-[d]	-[d]
			1695	42.2	1695	38.4	3378	50.9	1695	48.4	1696	56.8	1697	64.5
			1686	33.4	1683	41.7	3351	49.1	1683	51.6	1684	43.2	1686	35.5
4	H	Cl	-[a]	-	1705	25.1	-	-[d]	1703	14.7	1703	18.9	1704	13.8
			-	-	1696	40.5	3378	59.8	1691	68.9	1692	62.9	1693	78.9
			-	-	1682	34.6	3349	40.2	1676	16.4	1679	18.2	1676	7.3
5	H	Br	-[a]	-	1704	18.4	-	-[d]	1701	16.7	1702	21.1	1703	23.4
			-	-	1696	43.9	3377	59.4	1689	71.6	1692	61.1	1693	61.9
			-	-	1684	37.7	3349	40.6	1670	11.7	1680	17.8	1682	14.7
6	OMe	H	1697	24.1	1692	29.0	3367	30.8	1684	55.3	1685	61.8	1686	77.6
			1683	75.9	1679	71.0	3341	69.2	1674	44.7	1674	38.2	1675	22.4
7	Cl	H	1703	25.9	1699	37.7	3378	43.0	1694	57.2	1695	65.6	1696	81.0
			1790	74.1	1686	62.3	3353	57.0	1683	42.8	1684	34.4	1685	19.0

ε Relative permittivity.

[a] Compound not soluble in this solvent.

[b] Intensity of each component of the carbonyl doublet or triplet expressed in percentage of integrated absorbance.

[c] First overtone.

[d] The highest triplet frequency component is absent.

Table 4

Experimental frequencies (ν, cm^{-1}) and intensities of the carbonyl stretching bands in the IR spectra of 2-(deutero)-2-(methoxy)-2-(4-substituted-phenylsulfanyl)-acetophenones 4'-Y-PhC(O)CD[OMe][SPh-4-X] (**1a-5a**), in solvents of increasing relative permittivity

Comp.	**Y**	**X**	*n*-C_6H_{14} (ε = 1.9)		CCl_4 (ε = 2.2)				$CHCl_3$ (ε = 4.8)		CH_2Cl_2 (ε = 9.1)		CH_3CN (ε = 38)	
			ν	P[a]	ν	P	2ν[b]	P	ν	P	ν	P	ν	P
1a	H	OMe	-[c]	-	1698	34.2	3376	44.9	1689	83.4	1689	85.9	1692	89.2
			-	-	1683	65.8	3347	55.1	1674	16.6	1673	14.1	1679	10.8
2a	H	Me	1700	34.6	1697	36.3	3377	49.2	1690	70.3	1691	71.2	1693	78.3
			1687	65.4	1683	63.7	3348	50.8	1682	29.7	1680	28.8	1687	21.7
3a	H	H	1702	28.3	1698	38.9	3379	41.9	1691	67.7	1692	73.6	1694	80.1
			1687	71.7	1684	61.1	3351	58.1	1679	32.3	1679	26.4	1685	19.9
4a	H	Cl	-[c]	-	1698	36.4	3378	38.8	1690	77.1	1692	74.9	1692	87.2
			-	-	1685	63.6	3351	61.2	1674	25.1	1678	25.1	1680	12.8
5a	H	Br	-[c]	-	1697	36.0	3378	43.7	1690	71.6	1692	72.4	1693	78.3
			-	-	1684	64.0	3352	56.3	1673	28.4	1677	27.6	1675	21.7

ε Relative permittivity

[a] Intensity of each component of the carbonyl doublet expressed in percentage of integrated absorbance.

[b] First overtone.

[c] compound not soluble in this solvent

Table 5

Experimental ν_{CO} stretching frequencies ($\nu_{n/m}$, cm^{-1}) and the unperturbed frequencies ($\nu^0_{n/m}$, cm^{-1}) (**1**-**5**) along with the highest doublet frequency component [$\nu_{CO(C-D)}$, cm^{-1}] of the corresponding deuterated compounds (**1a**-**5a**)

Comp.	**1**		**1a**	**2**		**2a**	**3**		**3a**	**4**		**4a**	**5**		**5a**
Solvent	$\nu_{n/m}$	$\nu^0_{n/m}$	$\nu_{CO(C-D)}$	$\nu_{n/m}$	$\nu^0_{n/m}$	$\nu_{CO(C-D)}$	$\nu_{n/m}$	$\nu^0_{n/m}$	$\nu_{CO(C-D)}$	$\nu_{n/m}$	$\nu^0_{n/m}$	$\nu_{CO(C-D)}$	$\nu_{n/m}$	$\nu^0_{n/m}$	$\nu_{CO(C-D)}$
***n*-C_6H_{14}**	--[a]	--	--	1708.2 1697.9	1703.8 1702.3	 1700.4	1708.4 1695.2	1703.6 1700.0	 1702.2	--[a]	--	--	--[a]	--	--
CCl_4	1704.8[b] 1694.7[c]	1702.4[d] 1697.2[e]	 1697.5[f]	1705.1 1695.7	1701.3 1699.4	 1697.2	1704.3 1694.5	1700.9 1697.8	 1697.7	1705.3 1695.5	1701.6 1699.3	 1697.6	1704.4 1696.1	1702.4 1698.2	 1697.3
$CHCl_3$	--[a]	--	--	--[a]	--	--	--[a]	--	--	1702.7 1690.5	1700.6 1692.6	 1690.1	1701.4 1689.4	1699.5 1691.3	 1690.0
CH_2Cl_2	1703.0 1691.2	1702.0 1692.2	 1688.8	--[a]	--	--	--[a]	--	--	1702.5 1692.1	1700.1 1694.5	 1691.6	1701.7 1691.8	1699.4 1694.2	 1692.0
CH_3CN	--[a]	--	--	--[a]	--	--	--[a]	--	--	1703.6 1693.0	1702.0 1694.6	 1692.4	1702.8 1692.9	1700.2 1695.6	 1692.6

[a] For details see **Tables 3** and **4**.

[b,c] Refers to the frequencies of the experimental highest and medium triplet ν_{CO} stretching perturbed frequencies.

[d,e] Refers to the unperturbed frequencies corrected for the shift caused by Fermi Resonance.

[f] Refers to single ν_{CO} frequency of the corresponding methyne deuterated compounds.

Note: the values for frequencies are presented as fractionated numbers reflecting in more accurate unperturbed levels.

Table 6

Relative energy (E, kcal mol^{-1}), dipole moment (μ, D), carbonyl harmonic frequencies (ν, cm^{-1}), selected dihedral angles (°) optimized for the minimum energy conformations of PhC(O)CH[OMe][SPh-4-X] (**1**, **2**, **4** and **5**), 4'-Y-PhC(O)CH[OMe][SPh] (**6**, **3** and **7**) and PhC(O)C[D][OMe][SPh] (**3a**) at the B3LYP/6-31+G(d,p) level and the X-ray geometrical data of **6**.

Comp	X	Conf.[a]	E[b]	P[c] (%)	μ	ν_{CO}	Dihedral angles[d]							
							α	β	ϕ	δ	α'	β'	γ'	ϕ'
1	OMe	c_1	1.67	4.5	1.06	1758.4	-25.9	-165.0	71.4	-0.2	100.1	-51.1	-72.9	71.9
		c_2	0	74.8	3.85	1737.7	131.4	-162.8	-119.7	-3.8	-103.5	117.3	-67.6	75.0
		c_3	0.76	20.7	1.75	1734.5	126.2	-74.6	-83.6	3.8	-110.8	150.8	-101.7	162.7
2	Me	c_1	1.93	3.2	1.82	1758.8	-26.0	-164.4	71.2	1.6	100.1	-51.5	-70.9	72.3
		c_2	0	83.6	2.43	1734.8	131.8	-162.7	-120.0	-3.7	-103.3	116.8	-60.0	75.1
		c_3	1.09	13.2	2.47	1732.8	126.1	-73.6	-81.5	3.1	-110.8	153.1	-105.1	163.8
4	Cl	c_1	1.72	4.6	4.16	1758.5	-25.2	-164.4	73.5	-0.4	101.0	-49.4	-56.2	72.1
		c_2	0	83.3	3.12	1734.3	134.3	-161.9	-125.2	-4.7	-101.2	111.4	-54.1	75.9
		c_3	1.14	12.1	2.58	1736.3	126.4	-73.0	-81.4	3.1	-110.6	153.0	-109.0	164.4
5	Br	c_1	1.66	5.0	4.12	1758.2	-24.5	-164.9	74.4	-5.8	101.8	-48.4	-54.6	71.8
		c_2	0	82.9	3.08	1733.8	133.9	-161.9	-125.9	-3.7	-101.7	110.7	-53.3	76.1
		c_3	1.28	12.1	2.53	1736.6	126.1	-73.3	-81.9	3.5	-111.0	152.6	-110.2	164.2

[a] Conformer assignment.

[b] Relative energy.

[c] Molar fraction in percentage.

[d] See scheme 1.

Table 6 (continuation)

Comp	Y	Conf.[a]	E[b]	P[c] (%)	μ	ν_{CO}	Dihedral angles[d]							
							α	β	ϕ	δ	α'	β'	γ'	ϕ'
6	OMe	c_1	2.10	2.4	2.90	1751.0	-24.4	-164.4	74.4	0.3	102.1	-48.7	-58.5	71.6
		c_2	0	84.4	1.33	1724.8	133.8	-161.7	-125.4	-3.4	-101.7	111.2	-53.2	75.9
		c_3	1.10	13.2	1.91	1726.2	126.9	-73.6	-82.0	3.3	-110.1	152.4	-108.0	163.8
3	H	c_1	2.00	2.9	2.38	1759.6	-24.3	-164.4	73.7	0.2	102.1	-49.4	-56.0	71.8
		c_2	0	85.9	2.25	1735.5	133.3	-161.9	-123.7	-4.2	-102.1	113.1	-54.6	75.9
		c_3	1.21	11.2	2.15	1736.2	125.7	-73.3	-83.3	4.0	-111.2	151.2	-108.7	164.1
3a	H(D)[e]	c_1	2.03	2.8	2.38	1758.2	-24.3	-164.4	73.7	0.2	102.1	-49.4	-56.0	71.8
		c_2	0	86.2	2.25	1733.3	133.3	-161.9	-123.7	-4.2	-102.1	113.1	-54.6	75.9
		c_3	1.22	11.0	2.15	1733.9	125.7	-73.3	-83.3	4.0	-111.2	151.2	-108.7	164.1
7	Cl	c_1	2.19	2.1	1.67	1760.0	-24.8	-164.8	73.3	2.2	101.5	-49.5	-61.3	71.6
		c_2	0	86.7	3.23	1736.3	133.2	-162.0	-124.2	-3.5	-102.4	112.9	-55.9	76.0
		c_3	1.21	11.1	2.91	1736.5	126.2	-74.3	-83.0	4.0	-110.9	151.8	-106.7	163.4
6	X-ray	-	-	-	-	-	-18.3(2)	-171.88(14)	71.19(12)	-27.4(2)	106.39(15)	-49.65(11)	-62.41(15)	68.20(17)
1[f]		-	-	-	-	-	19.8(4)	161.9(3)	-74.1(3)	-0.6(4)	-104.5(3)	46.6(3)	-101.2(3)	-76.7(3)
2[g]		-	-	-	-	-	-18.2(5)	-164.3(3)	63.2(4)	4.9(6)	105.9(4)	-57.9(3)	-83.1(4)	74.4(4)
4[h]		-	-	-	-	-	19.3(7)	163.9(5)	-63.7(4)	-2.9(8)	-105.1(5)	57.3(5)	80.5(5)	-75.3(6)

[a] Conformer assignment.
[b] Relative energy.
[c] Molar fraction in percentage.
[d] See scheme 1.
[e] Refers to the deuterated analogue **3a**
[f,g,h] From refs. [11], [10], [9], respectively

Table 7

Relative energies (E, kcal mol^{-1}), carbonyl harmonic frequencies ($\nu_{C=O}$, cm^{-1}) and dipole moments (μ, D) optimized for different conformers of **1**-7 at the B3LYP/6-31+G(d,p) level of theory including the solvent effect PCM method.

Comp.	X	Conf.[a]	*n*-C_6H_{14}				CCl_4				$CHCl_3$				CH_2Cl_2				CH_3CN			
			E[b]	P[c]	$\nu_{C=O}$	μ[d]	E	P	$\nu_{C=O}$	μ	E	P	$\nu_{C=O}$	μ	E	P	$\nu_{C=O}$	μ	E	P	$\nu_{C=O}$	μ
1	OMe	c_1	1.14	10.3	1747.5	1.39	1.02	12.4	1745.1	1.50	0.80	26.6	1734.6	2.04	0.06	42.4	1728.2	2.31	0	61.6	1721.2	2.63
		c_2	0	70.5	1729.1	4.41	0	69.3	1727.1	4.53	0	58.4	1718.7	5.00	0	46.9	1713.7	5.20	0.38	32.4	1703.4	4.61
		c_3	0.77	19.2	1723.7	1.84	0.79	18.2	1721.5	1.85	0.47	15.1	1713.2	1.89	0.87	10.7	1708.8	1.92	1.37	6.0	1704.5	1.96
2	Me	c_1	1.43	7.2	1747.6	2.11	1.26	9.3	1745.0	2.18	0.52	26.3	1734.4	2.49	0.10	42.2	1727.8	2.70	0	64.6	1720.7	2.95
		c_2	0	80.0	1726.6	2.83	0	77.7	1724.9	2.93	0	63.4	1717.1	3.28	0	50.2	1712.5	3.44	0.44	30.7	1707.7	3.60
		c_3	1.08	12.8	1722.5	2.75	1.06	13.0	1720.4	2.81	1.07	10.3	1712.1	3.05	1.12	7.6	1707.6	3.18	1.55	4.7	1703.1	3.31
4	Cl	c_1	1.26	9.5	1748.8	4.57	1.09	12.2	1746.1	4.70	0.40	31.1	1735.4	5.20	0	50.1	1729.2	5.50	0	71.6	1722.5	5.81
		c_2	0	79.6	1728.5	3.32	0	77.2	1726.5	3.38	0	60.9	1719.4	3.60	0.07	44.3	1715.4	3.75	0.61	25.4	1711.3	3.90
		c_3	1.18	10.9	1726.0	2.88	1.18	10.6	1723.6	2.95	1.20	8.0	1715.4	3.20	1.30	5.6	1710.6	3.35	1.87	3.0	1706.0	3.50
5	Br	c_1	1.29	9.0	1748.9	4.59	1.14	11.4	1746.0	4.72	0.42	30.2	1736.2	5.07	0	49.9	1730.1	5.38	0	75.8	1723.2	5.71
		c_2	0	80.2	1728.1	3.27	0	78.1	1726.3	3.33	0	61.7	1719.5	3.56	0.07	44.4	1715.5	3.70	0.62	25.0	1711.4	3.84
		c_3	1.19	10.8	1726.0	2.85	1.18	10.6	1723.7	2.93	1.21	8.0	1715.6	3.17	1.28	5.7	1710.5	3.23	1.85	3.2	1706.4	3.37

[a] Conformer attribution.

[b] Relative energy.

[c] Molar fraction in percentage.

[d] Dipole moment.

Table 7 (continuation)

Comp.	Y	Conf.[a]	*n*-C_6H_{14}				CCl_4				$CHCl_3$				CH_2Cl_2				CH_3CN			
			E[b]	P[c]	$\nu_{C=O}$	μ[d]	E	P	$\nu_{C=O}$	μ	E	P	$\nu_{C=O}$	μ	E	P	$\nu_{C=O}$	μ	E	P	$\nu_{C=O}$	μ
6	OMe	c_1	1.69	4.7	1739.0	3.21	1.52	6.2	1736.1	3.29	0.80	18.2	1724.3	3.48	0.29	34.6	1717.5	3.69	0	58.7	1710.3	3.91
		c_2	0	82.5	1716.7	1.47	0	80.9	1714.7	1.50	0	70.7	1707.9	1.72	0	56.6	1703.3	1.85	0.29	35.7	1698.8	1.96
		c_3	1.10	12.8	1714.6	2.16	1.09	12.9	1711.9	2.22	1.09	11.1	1703.4	2.50	1.10	8.8	1698.4	2.57	1.39	5.6	1694.1	2.78
3	H	c_1	1.48	6.6	1749.5	2.58	1.35	8.1	1746.9	2.66	0.74	20.2	1736.2	3.01	0.26	36.2	1729.8	3.30	0	60.0	1722.7	3.57
		c_2	0	81.4	1729.2	2.75	0	79.8	1727.4	2.83	0	70.2	1719.7	3.15	0	56.1	1715.2	3.32	0.31	35.3	1710.8	3.49
		c_3	1.13	12.0	1725.1	2.43	1.12	12.1	1722.9	2.48	1.18	9.6	1714.7	2.81	1.18	7.7	1710.2	2.95	1.51	4.7	1706.0	3.08
7	Cl	c_1	1.68	4.9	1750.2	1.93	1.51	6.5	1747.7	2.00	0.69	21.6	1737.1	2.31	0.15	40.8	1730.9	2.51	0	65.8	1724.0	2.74
		c_2	0	84.7	1730.0	3.71	0	83.1	1728.3	3.80	0	69.0	1721.5	4.12	0	52.1	1717.9	4.31	0.46	30.1	1713.7	4.50
		c_3	1.24	10.4	1727.0	3.20	1.23	10.4	1725.2	3.32	1.18	9.4	1717.2	3.51	1.18	7.1	1712.7	3.61	1.64	4.1	1708.7	3.78

[a] Conformer attribution.
[b] Relative energy.
[c] Molar fraction in percentage.
[d] Dipole moment.

Table 8

Harmonic, anharmonic unperturbed and perturbed frequencies (cm^{-1}) of the $\nu_{CO}(15)$, $\delta_{CH}(32)$ and the skeletal (72) vibrational modes and mechanical ν_{CO} anharmonicity (cm^{-1}) of **3** obtained at the B3LYP / 6-31+G(d,p) level in vacuum.

	Conformer[a]						
	c1		*c2*			*c3*	
VibrationalMode	Harmonic	Anharmonic[b]	Harmonic	Anharmonic[b]	Fermi[c]	Harmonic	Anharmonic[b]
Mode 15 $\nu_{C=O}$							
Fundamental	1760.7	1728.1	1735.6	1708.2	1709.0	1736.2	1705.9
Overtone	3521.4	3435.9	3471.2	3397.3	-	3472.4	3392.4
$2\omega e\chi e$	0	20.3	0	19.1	-	0	19.4
Mode 32 δ_{C-H}	1273.1	1235.8	1296.8	1264.6	-	1286.8	1262.2
Modo 72 Skeletal	430.3	422.8	441.3	437.3	-	425.0	413.2
72+32[d]	1703.5	1658.6	1737.8	1701.9	1696.1	1708.7	1675.4

[a] See scheme 1 and Table 6.

[b] Unperturbed modes

[c] Fermi perturbed modes.

[d] Resulting combination mode.

Table 9

Potential energy distribution of conformers c_1, c_2 and c_3, of compound **3** obtained at B3LYP/6-31+G(d,p) level.

Conf.	<EPm>[a]	Normal mode[b]	ν[c]	Mixing coordinates[d]	%[e,f]
c_1	59.15	15 ν_{CO}	1760.7	$\nu_{(O1=C2)}$	90
		32 δ_{CH}	1273.1	$\tau_{(H4-C3-O5-C6)}$	25
				$\nu_{(C2-C22)}$	18
		72 Skeletal	430.3	$\tau_{(C22-C31-C29-C27)}-\tau_{(C25-C27-C29-C31)}$	17
				$\delta_{(C3-C2-C22)}-\delta_{(C3-O5-C6)}+\delta_{(C22-C2-O1)}+\delta_{(C22-C31-C29)}$	13
				$\delta_{(O5-C3-S10)}$	11
				$\omega_{(S10-C12-C16-C11)}+\tau_{(C12-C14-C16-C18)}$	11
c_2	60.83	15 ν_{CO}	1735.6	$\nu_{(O1=C2)}$	87
		32δ_{CH}	1296.8	$\nu_{(C2-C22)}-\nu_{(C2-C3)}$	46
				$\delta_{(H32-C31-C29)}+\delta_{(H24-C23-C25)}+\delta_{(H26-C25-C27)}-\delta_{(H30-C29-C31)}$	10
		72 Skeletal	441.3	$\nu_{(S10-C11)}+\nu_{(C18-C20)}+\nu_{(C11-C20)}+\nu_{(C2-C22)}$	30
				$\delta_{(C14-C16-C18)}$	15
				$\tau_{(C14-C16-C18-C20)}-\omega_{(S10-C12-C20-C11)}-\tau_{(C12-C14-C16-C18)}$	11
c_3	59.03	15 ν_{CO}	1736.2	$\nu_{(O1=C2)}$	88
		32δ_{CH}	1286.8	$\nu_{(C2-C22)}$	38
				$\tau_{(H7-C6-O5-C3)}-\tau_{(H4-C3-O5-C6)}$	14
		72 Skeletal	425.0	$\nu_{(S10-C11)}$	23
				$\delta_{(C14-C16-C18)}$	15

[a] <EPm> parameter should be between 55.0 and 85.0[46].
[b] Analyzed Normal mode.
[c] Harmonic frequency.
[d] Vibrational modes coordinates involved on the resulting normal modes frequencies. Plus and minus signs design the phase
[e] Percentage of the coordinate on the normal mode of vibration.
[f] Coordinates with less than 10% of contribution on the normal modes are not listed.

Table 10

Solvent effect on anharmonic frequencies (cm^{-1}) of unperturbed vibrational modes and difference between the carbonyl stretching band and the combination band (cm^{-1}) of **3** obtained by PCM calculations at B3LYP/6-31+G(d,p) level.

Conf.[a]	Normal mode			
		Vacuum	CCl_4	CH_3CN
c1	15 ($\nu_{C2=O1}$)	1728.1	1714.7	1697.1
	32 (δ_{C3-H4})	1235.8	1296.7	1299.4
	72 (skeletal)	422.8	423.8	431.4
	32+72[b]	1658.6	1720.5	1730.8
	$\Delta\nu$[c]	69.5	-5.8	-33.7
c2	15 ($\nu_{C2=O1}$)	1708.2	1696.5	1676.4
	32 (δ_{C3-H4})	1264.6	1268.8	1291.8
	72 (skeletal)	437.3	439.2	438
	32+72	1701.9	1708	1729.8
	$\Delta\nu$	6.3	-11.5	-53.4
c3	15 ($\nu_{C2=O1}$)	1705.9	1700.5	1668.1
	32 (δ_{C3-H4})	1262.2	1256.4	1257.9
	72 (skeletal)	413.2	413.4	415.3
	32+72	1675.4	1669.8	1673.2
	$\Delta\nu$	30.5	30.7	-5.1

[a] Conformer assignment.
[b] Combination band (sum).
[c] Difference between the ν_{CO} and the combination band frequencies [15-(72+32)].

Table 11

ChelpG charges (e) at selected atoms obtained at the B3LYP/6-31+G(d,p) level for 4'-Y-PhC(O)CH[OMe][SPh-4-X] (**1-7**)

Comp.	Y	X	Conf	$O(1)_{[CO]}$	$C(2)_{[CO]}$	C(3)	O(5)	S(10)	$H(4)_{[CH]}$	$H(7)_{[OCH3]}$	$H(32)_{[o\text{-}PhC(O)]}$
1	H	OMe	c_1	-0.43	0.20	0.64	-0.52	-0.39	-0.020	-0.040	0.129
			c_2	-0.48	0.34	0.51	-0.51	-0.37	-0.026	-0.037	0.160
			c_3	-0.52	0.52	0.22	-0.38	-0.34	0.017	0.040	0.054
2	H	Me	c_1	-0.42	0.22	0.59	-0.51	-0.39	-0.005	0.039	0.123
			c_2	-0.47	0.32	0.50	-0.52	-0.37	-0.017	-0.046	0.163
			c_3	-0.52	0.53	0.20	-0.37	-0.34	0.019	0.038	0.056
3	H	H	c_1	-0.41	0.22	0.56	-0.50	-0.36	0.009	-0.040	0.111
			c_2	-0.47	0.32	0.51	-0.52	-0.36	-0.019	-0.044	0.169
			c_3	-0.52	0.49	0.28	-0.38	-0.35	-0.008	0.040	0.052
4	H	Cl	c_1	-0.41	0.25	0.50	-0.49	-0.35	0.036	-0.042	0.180
			c_2	-0.47	0.33	0.48	-0.50	-0.34	-0.010	-0.041	0.182
			c_3	-0.52	0.53	0.23	-0.37	-0.34	0.006	0.040	0.048
5	H	Br	c_1	-0.42	0.27	0.47	-0.50	-0.35	0.050	-0.038	0.101
			c_2	-0.47	0.31	0.53	-0.52	-0.35	-0.023	-0.047	0.169
			c_3	-0.51	0.50	0.27	-0.37	-0.34	-0.007	0.033	0.044
6	OMe	H	c_1	-0.44	0.27	0.55	-0.50	-0.37	0.006	-0.038	0.125
			c_2	-0.49	0.36	0.46	-0.51	-0.35	-0.007	-0.045	0.180
			c_3	-0.55	0.56	0.26	-0.38	-0.36	-0.003	0.041	0.061
7	Cl	H	c_1	-0.42	0.26	0.50	-0.49	-0.36	0.022	-0.039	0.133
			c_2	-0.48	0.38	0.42	-0.49	-0.34	0.006	-0.037	0.185
			c_3	-0.54	0.57	0.20	-0.37	-0.35	0.014	0.039	0.074

Table 12

Selected interatomic distances (Å) for the minimum energy conformations of 4'-Y-PhC(O)CH[OMe][SPh-4-X] (**1-7**) at the B3LYP/6-31+G(d,p) level and the intramolecular X-ray contacts for **6**.

Comp	Y	X	Conf.[a]	$O_1 \cdots O_5$	Δl[c]	$O_1 \cdots H_4$	Δl	$O_5 \cdots H_{32}$	Δl	$S_{10} \cdots H_7$	Δl	$S_{10} \cdots H_{32}$	Δl
1	H	OMe	c_1	2.65	-0.39	3.23	-	4.00	-	2.93	-0.07	3.16	-
			c_2	3.38	-[d]	2.42	-0.30	2.37	-0.35	2.97	-0.03	2.99	-0.01
			c_3	3.43	-	2.41	-0.31	2.39	-0.33	4.22	-	2.95	-0.05
2	H	Me	c_1	2.65	-0.39	3.23	-	4.01	-	2.93	-0.07	3.12	-
			c_2	3.39	-	2.41	-0.31	2.37	-0.35	2.96	-0.04	3.00	-
			c_3	3.42	-	2.41	-0.31	2.40	-0.32	4.23	-	2.94	-0.06
3	H	H	c_1	2.64	-0.40	3.22	-	4.02	-	2.93	-0.07	3.10	-
			c_2	3.40	-	2.41	-0.31	2.36	-0.36	2.96	-0.06	3.02	-
			c_3	3.42	-	2.41	-0.31	2.39	-0.33	4.23	-	2.94	-0.06
4	H	Cl	c_1	2.64	-0.40	3.23	-	4.00	-	2.93	-0.07	3.14	-
			c_2	3.40	-	2.41	-0.31	2.35	-0.37	2.95	-0.05	3.04	-
			c_3	3.43	-	2.41	-0.31	2.40	-0.32	4.23	-	2.94	-0.06
5	H	Br	c_1	2.64	-0.40	3.22	-	3.99	-	2.92	-0.08	3.25	-
			c_2	3.40	-	2.41	-0.31	2.35	-0.37	2.95	-0.05	3.05	-
			c_3	3.43	-	2.41	-0.31	2.40	-0.32	4.23	-	2.94	-0.06
6	OMe	H	c_1	2.64	-0.40	3.22	-	4.03	-	2.92	-0.08	3.10	-
			c_2	3.40	-	2.41	-0.31	2.35	-0.37	2.94	-0.06	3.06	-
			c_3	3.43	-	2.41	-0.31	2.39	-0.33	4.23	-	2.96	-0.04
7	Cl	H	c_1	2.64	-0.40	3.22	-	4.03	-	2.93	-0.07	3.08	-
			c_2	3.39	-	2.42	-0.30	2.35	-0.37	2.96	-0.06	3.03	-
			c_3	3.42	-	2.42	-0.30	2.39	-0.33	4.23	-	2.95	-0.05
6	OMe	H	X-ray	2.6157(17)	-0.42	3.05	-	4.02	-	2.85	-0.13	3.60	-
	ΣvdWr[b]			3.04		2.72		2.72		3.00		3.00	

[a] Conformer designation.

[b] Sum of the van der Waals radii.

[c] Difference between nonbonded atoms distance and the sum of the van der Waals radii.

[d] Interatomic distance larger than the sum of the van der Waals radii.

Table 13

Comparison of significant NBO energies (kcal mol^{-1}) of the interacting orbitals for the c_1, c_2 and c_3 conformers of 4'-Y-PhC(O)CH[OMe][SPh-4-X] **1-7** at the B3LYP/6-31+G(d,p) level

Orbitals	X = OMe (**1**)			X = Me (**2**)			X = Cl (**4**)			X = Br (**5**)		
	c_1	c_2	c_3	c_1	c_2	c_3	c_1	c_2	c_3	c_1	c_2	c_3
$\pi_{C22=C31} \rightarrow \pi^*_{C2=O1}$	20.4	22.8	23.0	20.4	23.0	23.1	20.8	23.4	23.3	20.6	23.4	23.2
$LP_{O1} \rightarrow \sigma^*_{C2-C3}$	23.4	21.0	21.3	23.5	21.0	21.4	23.7	20.9	21.5	23.7	20.9	21.6
$LP_{O1} \rightarrow \sigma^*_{C2-C22}$	20.0	19.2	19.3	20.0	19.2	19.3	19.8	19.0	19.3	19.8	19.0	19.3
$LP_{O5} \rightarrow \sigma^*_{C3-S10}$	15.8	15.0	1.2	15.9	15.1	1.3	16.0	15.4	1.3	15.9	15.4	1.3
$LP_{O5} \rightarrow \sigma^*_{C2-C3}$	1.8	1.7	9.3	1.8	1.7	9.2	1.8	1.7	9.3	1.8	1.7	9.3
$\sigma_{C3-S10} \rightarrow \sigma^*_{O5-C6}$	-[a]	-	2.2	-	-	2.2	-	-	2.2	-	-	2.2
$\sigma_{O5-C6} \rightarrow \sigma^*_{C3-S10}$	-	-	2.5	-	-	2.5	-	-	2.6	-	-	2.6
$LP_{S10} \rightarrow \sigma^*_{C3-O5}$	6.5	5.8	8.9	6.5	5.7	8.9	6.5	4.9	8.7	6.6	4.8	8.7
$LP_{S10} \rightarrow \sigma^*_{C2-C3}$	2.5	2.2	-	2.5	2.3	-	2.5	2.5	-	2.4	2.5	-
$LP_{S10} \rightarrow \pi^*_{C11=C12}$	1.7	3.3	1.4	2.6	5.5	1.4	6.5	7.5	1.9	7.0	7.8	2.2
$LP_{O5} \rightarrow \pi^*_{O1=C2}$	-	-	1.1	-	-	1.1	-	-	1.0	-	-	1.0
$LP_{S10} \rightarrow \pi^*_{O1=C2}$	1.6	2.2	0.7	1.7	2.2	0.6	1.5	2.4	0.5	1.5	2.4	0.6
$\pi_{C2=O1} \rightarrow \sigma^*_{C3-O5}$	-	2.0	2.3	-	2.0	2.3	-	1.8	2.3	-	1.9	2.3
$\pi_{C2=O1} \rightarrow \sigma^*_{C3-S10}$	2.4	2.0	1.8	2.4	2.1	1.8	2.4	2.1	1.8	2.4	2.1	1.8
$\sigma_{C3-O5} \rightarrow \pi^*_{O1=C2}$	-	0.9	1.0	-	0.9	1.0	-	0.8	1.0	-	0.8	1.0
$\sigma_{C3-S10} \rightarrow \pi^*_{O1=C2}$	6.0	5.0	4.4	5.8	5.0	4.3	5.7	5.2	4.3	5.8	5.2	4.3
$LP_{O1} \rightarrow \sigma^*_{C23-H24}$	0.5	-	-	0.5	-	-	0.5	-	-	-	-	-
$LP_{O5} \rightarrow \sigma^*_{C3-H4}$	3.5	3.3	3.2	3.5	3.3	3.3	3.5	3.2	3.4	3.5	3.2	3.3
$LP_{O5} \rightarrow \sigma^*_{C31-H32}$	-	0.6	0.9	-	0.6	0.8	-	0.7	0.8	-	0.8	0.8
$LP_{S10} \rightarrow \sigma^*_{C6-H7}$	0.8	0.6	-	0.8	0.6	-	0.8	0.7	-	0.8	0.7	-
ΣE	106.9	107.6	104.5	107.9	110.2	104.5	112.0	112.2	105.2	111.8	112.6	105.5

[a] Interaction energy lower than 0.5 kcal mol^{-1}.

Table 13 (continuation)

Orbitals	Y = OMe (**6**)			Y = H (**3**)			Y = Cl (**7**)		
	c_1	c_2	c_3	c_1	c_2	c_3	c_1	c_2	c_3
$\pi_{C22=C31} \rightarrow \pi^*_{C2=O1}$	22.8	25.0	24.9	20.6	23.1	23.1	20.3	22.9	22.8
$LP_{O1} \rightarrow \sigma^*_{C2-C3}$	23.9	20.9	21.6	23.7	22.9	21.4	23.7	20.9	21.4
$LP_{O1} \rightarrow \sigma^*_{C2-C22}$	19.7	18.7	19.1	19.9	19.1	19.3	20.3	19.3	19.5
$LP_{O5} \rightarrow \sigma^*_{C3-S10}$	15.7	15.0	1.3	15.7	15.1	1.3	15.9	15.0	1.3
$LP_{O5} \rightarrow \sigma^*_{C2-C3}$	1.8	1.7	9.1	1.8	1.7	9.2	1.8	1.7	9.3
$\sigma_{C3-S10} \rightarrow \sigma^*_{O5-C6}$	-[a]	-	2.2	-	-	2.2	-	-	2.2
$\sigma_{O5-C6} \rightarrow \sigma^*_{C3-S10}$	-	-	2.5	-	-	2.5	-	-	2.5
$LP_{S10} \rightarrow \sigma^*_{C3-O5}$	6.7	4.9	8.8	6.6	5.2	8.9	6.6	5.1	8.9
$LP_{S10} \rightarrow \sigma^*_{C2-C3}$	2.5	2.6	-	2.5	2.5	-	2.5	2.5	-
$LP_{S10} \rightarrow \pi^*_{C11=C12}$	5.8	7.7	1.7	6.5	7.2	1.8	5.0	6.7	1.4
$LP_{O5} \rightarrow \pi^*_{O1=C2}$	-	-	1.0	-	-	1.0	-	-	1.1
$LP_{S10} \rightarrow \pi^*_{O1=C2}$	1.4	2.3	0.6	1.5	2.3	0.6	1.5	2.4	0.6
$\pi_{C2=O1} \rightarrow \sigma^*_{C3-O5}$	-	1.9	2.3	-	1.9	2.3	-	1.9	2.3
$\pi_{C2=O1} \rightarrow \sigma^*_{C3-S10}$	2.4	2.1	1.8	2.4	2.1	1.8	2.4	2.1	1.8
$\sigma_{C3-O5} \rightarrow \pi^*_{O1=C2}$	-	0.8	1.0	-	0.9	1.0	-	0.9	1.0
$\sigma_{C3-S10} \rightarrow \pi^*_{O1=C2}$	5.5	5.1	4.3	5.6	5.1	4.3	5.7	5.2	4.4
$LP_{O1} \rightarrow \sigma^*_{C23-H24}$	0.5	-	-	0.5	-	-	0.5	-	-
$LP_{O5} \rightarrow \sigma^*_{C3-H4}$	3.5	3.2	3.4	3.5	3.2	3.4	3.6	3.2	3.3
$LP_{O5} \rightarrow \sigma^*_{C30-H31}$	-	0.7	0.9	-	0.7	0.9	-	0.7	0.9
$LP_{S10} \rightarrow \sigma^*_{C6-H7}$	0.8	0.7	-	0.8	0.6	-	0.8	0.7	-
ΣE	113.0	113.3	106.5	111.6	113.6	105.0	110.6	111.2	104.7

[a] Interaction energy lower than 0.5 kcal mol^{-1}.

Figure S1

Click here to download Supplementary Material: Fig S1.doc

Figure S2

Click here to download Supplementary Material: Fig S2.doc

Figure S3

Click here to download Supplementary Material: Fig S3.doc